

Single-atom nanozymes as promising catalysts for biosensing and biomedical applications

| | |
|-------------------------------|---|
| Journal: | <i>Inorganic Chemistry Frontiers</i> |
| Manuscript ID | QI-CFR-03-2023-000430.R1 |
| Article Type: | Chemistry Frontiers |
| Date Submitted by the Author: | 11-Apr-2023 |
| Complete List of Authors: | Xiao, Yaqian ; Hubei University of Chinese Medicine, School of Laboratory Medicine Hu, Xiao; Hubei University of Chinese Medicine, School of Laboratory Medicine Liu, Qiming; University of California Santa Cruz, Chemistry and Biochemistry Zhang, Yulin; Hubei University of Chinese Medicine, School of Laboratory Medicine Zhang, Guo-Jun; Hubei University of Chinese Medicine, School of Laboratory Medicine Chen, Shaowei; University of California Santa Cruz, Department of Chemistry and Biochemistry |
| | |

ARTICLE

Single-atom nanozymes as promising catalysts for biosensing and biomedical applications

Received 00th January 20xx,
Accepted 00th January 20xx

Xueqian Xiao^{a,#}, Xiao Hu^{a,#}, Qiming Liu^b, Yuling Zhang^a, Guo-Jun Zhang^{a,*}, Shaowei Chen^{b,*}

DOI: 10.1039/x0xx00000x

Nanozymes with intrinsic enzyme-like properties and excellent stability are promising alternatives to natural enzymes. Yet, the low density of active sites and unclear crystal structure has been the major obstacles that impede the progress. Single-atom nanozymes (SAzymes) have emerged as a unique system to mitigate these issues, due to maximal atomic utilization, well-defined electronic and geometric structures, and outstanding catalytic activity distinct from their nanosized counterparts. Furthermore, the homogeneously dispersed active sites and well-defined coordination structures provide rare pathways to shed light onto the catalytic mechanisms. In this review, we will summarize the latest progress in the rational design and engineering of SAzymes and their applications in biomedicine and biosensing. We will conclude the review with highlights of the remaining challenges and perspectives of this emerging technology.

Contents

| | |
|--|----|
| 1. Introduction | 1 |
| 2. Synthetic Strategies | 2 |
| 3. SAzyme Supports | 3 |
| 3.1 Carbon-based supports | 3 |
| 3.2 Noncarbon-based supports | 4 |
| 4. Enzymatic Activity of SAzymes | 5 |
| 4.1 Fe SAzymes | 5 |
| 4.2 Co SAzymes | 6 |
| 4.3 Zn SAzymes | 7 |
| 4.4 Pt SAzymes | 8 |
| 4.5 Other nanozymes | 8 |
| 4.6 Nonmetal dopants | 9 |
| 5. Biological and Medical Applications | 10 |
| 5.1 Biosensing | 10 |
| 5.2 Cancer diagnosis and therapy | 11 |
| 5.3 Antibacterial and antiviral activity | 12 |
| 5.4 Other applications | 13 |
| 6. Conclusion and Perspectives | 14 |

1. Introduction

Enzymes are biocatalysts produced by living cells that possess a high catalytic activity promoting specific biological reactions in the body and maintain cell life activities. Most enzymes are proteins (a small number are RNA), and their catalytic activities can be greatly impacted by the chemical environment, as the

enzymes are prone to degradation, and the high cost of preparation renders it difficult for large-scale production. To mitigate these issues, artificial enzymes have been attracting extensive attention as the stable and low-cost alternatives.^{1, 2} In 2007, Yan et al. found that Fe₃O₄ nanoparticles exhibited peroxidase (POD)-like activity and the optimal catalytic conditions were approximate to those of natural horseradish peroxidase (HRP), which was a significant breakthrough in the field of nanomaterials biocatalysis.³ Since then, the term "nanozyme" has attracted widespread attention,⁴⁻⁶ due largely to the high stability, low cost, tuneable catalytic activity, and ease of large-scale production.^{7, 8} There are three major types of nanozymes based on their substrates, carbon-based nanozymes, metal-based nanozymes, and metal oxide-based

^a School of Laboratory Medicine, Hubei University of Chinese Medicine, 16 Huangjia Lake West Road, Wuhan, Hubei 430065, China

^b Department of Chemistry and Biochemistry, University of California, 1156 High Street, Santa Cruz, California 95064, United States

* Corresponding authors: zhanggj@hbtcm.edu.cn, shaowei@ucsc.edu

These authors contributed equally to the work

nanozymes,⁹ featuring catalytic activities resembling those of natural enzymes like POD, oxidase (OXD), catalase (CAT), superoxide dismutase (SOD), glucose oxidase (GOx) and hydrolase.^{10–12} Thus far, nanozymes have been widely adopted in diverse fields, such as disease diagnosis and treatment, biosensing, food safety, environmental monitoring, chemical production, among others.^{13–15}

Whereas nanozymes may possess properties that are superior to those of natural enzymes, the catalytic activity and substrates affinity remain mostly subpar as compared to that of natural enzymes. This is mainly attributed to the low density of active sites in nanozymes, and the unclear crystal structure and complex elemental composition make it difficult to unravel the catalytic mechanisms.^{16, 17} To overcome these barriers, single-atom nanozymes (SAzymes) have emerged as a unique platform, where the catalytic activity can be enhanced by the maximal utilization of metal atoms and the well-defined atomic configuration offers unprecedented insights into the mechanistic origin.¹⁸

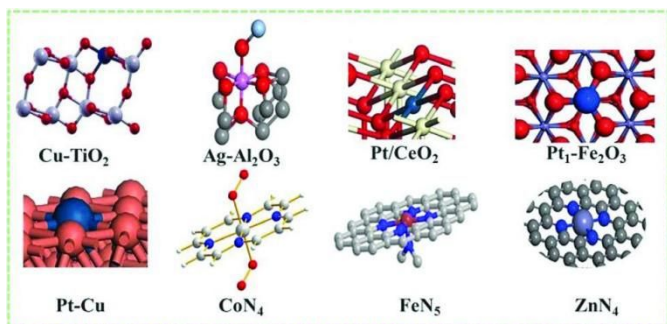
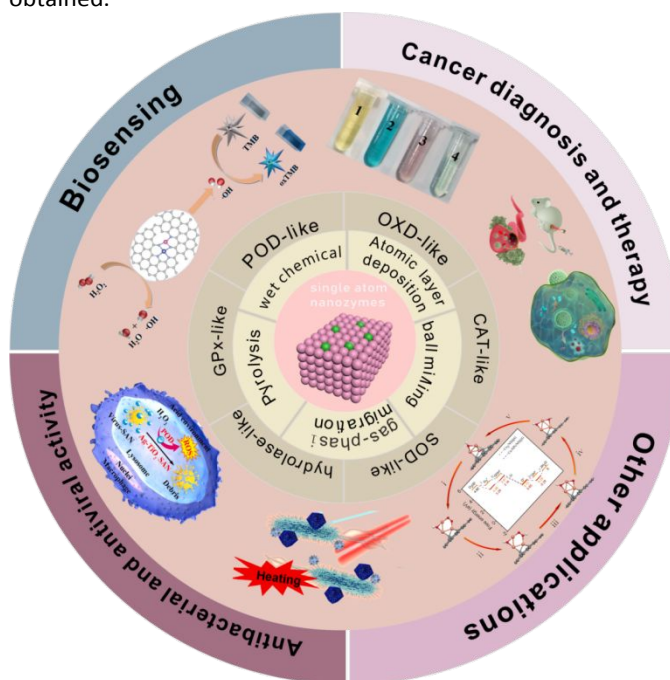


Figure 1. Representative SAzymes with metal centers homogeneously dispersed within a range of supporting scaffolds, such as carbon, metal oxides, and metals. Reproduced with permission from ref. 20, Copyright 2020, Royal Society of Chemistry.

In SAzymes, isolated metal atoms are anchored onto a select structural scaffold and the resultant coordination moiety serves as the active centers (**Figure 1**).^{19, 20} SAzymes combine the advantages of homogeneous catalysts and heterogeneous catalysts and may break the limitations in material design for unprecedented catalytic activity.^{21, 22} In most studies, SAzymes exhibit POD- and OXD-like activity,^{23–25} and can break down H_2O_2 to reactive oxygen molecules (ROS) that are potent agents in the inhibition of the growth of harmful cells such as bacteria and viruses.^{26–28} Meanwhile, by deliberate manipulation of the coordination structure between the metal atoms and the supports, the SAzyme active centers can be carefully tailored, leading to multienzyme catalytic activity for enzyme cascade reactions,^{29, 30} and a catalytic performance competitive to that of the natural enzyme.³¹ Meanwhile, the well-defined active sites and electronic properties render it possible to reveal the structure-activity correlation.^{32–34} In addition, the development of effective synthetic strategies, such as wet impregnation and high-temperature annealing, have made it possible for large-scale preparation of SAzymes with a high metal coverage and stable metal coordination structure, as compared to conventional synthesis methods.³⁵ The structural insights can also be exploited for the construction of relevant models for theoretical calculations

where further insights into the mechanistic origin can be obtained.³⁶



Scheme 1. Schematic illustration of SAzymes for a broad scope of biologically critical applications.

In this review, we will summarize the latest progress in the design and synthesis of SAzymes and their applications in biomedicines and biosensing, highlight the remaining challenges and put forward opportunities in future research (**Scheme 1**).

2. Synthetic Strategies

Experimentally, a range of structural parameters, in particular, the coordination configuration of the metal centers and the geometric structure of the supporting substrates, have been found to impact the catalytic performance of SAzymes. This may consist of the manipulation of the crystal plane, surface coating, elemental composition, heteroatom doping, selection of cofactor mimics, among others.³⁷ Thus far, a great many SAzymes have been successfully prepared via both bottom-up and top-down synthetic procedures. The former mainly involves atomic layer deposition (ALD),^{38, 39} ball milling,^{40, 41} wet Chemistry,^{42, 43} mass-selected soft landing,^{44, 45} and photochemical reduction,^{46, 47} while the latter entails high-temperature pyrolysis^{48, 49} and gas-phase migration^{50, 51}. Below is a summary of these synthetic methods.

Pyrolysis is a widely used method for the synthesis of SAzymes.⁵² Experimentally, a metal salt precursor is incorporated into a select organic matrix (typically containing nitrogen). The mixture is then pyrolyzed at elevated temperatures under an inert atmosphere, where the nitrogen atoms are doped into the resulting carbon scaffold and the metal atoms form an M-N-C coordination structure with the carbon and nitrogen atoms (e.g., M = Fe, Cu, Co, Zn, Mn,

etc.).⁵³ Among these, metal-organic frameworks (MOFs) are the commonly used support materials due to their structural diversity and functional tunability.⁵⁴ Under high temperature and inert atmosphere, the organic ligands are carbonized and the metal nodes within the MOFs are converted into metal sites uniformly dispersed within the carbon support. For example, zeolitic imidazole framework-8 (ZIF-8) has been used as a precursor for the preparation of Fe SAzymes consisting of FeN₄ and FeN₅ active sites through a melamine-mediated two-step pyrolysis strategy, where the coating of a SiO₂ shell inhibits nanoparticle aggregation during high-temperature pyrolysis (Figure 2).⁵⁵

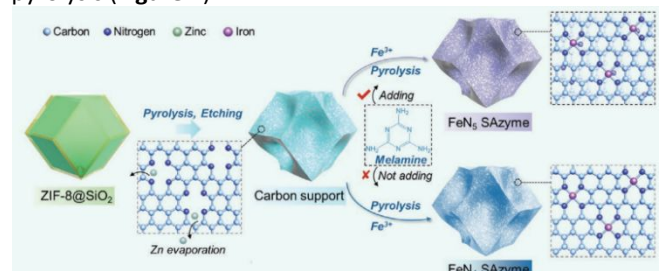


Figure 2. Schematic illustration of the synthesis of FeN₅ SAzyme from a ZIF-8 precursor. Reproduced with permission from ref. 55, copyright 2022, Wiley.

However, pyrolysis at high temperatures usually produces metal (oxide)-containing nanoparticles, resulting in a heterogeneous structure. Note that whereas the nanoparticles may be removed by, for instance, acid etching, the removal is generally incomplete.⁵⁶ In addition, during pyrolytic treatment of MOFs, the framework structure may collapse, leading to rearrangement of the carbon skeleton, which may complicate the structure and compromise the accessibility of the M-N-C moiety.

Wet-chemistry strategies have also been employed extensively for SAzyme synthesis.^{57, 58} In such procedures, metal-containing precursors are immobilized onto a suitable support via impregnation, co-precipitation, ion exchange or electrostatic absorption, followed by drying and calcination to remove the undesired ligands. In the wet-chemistry procedures, it is important to strengthen the interactions between the metal atoms and the support, and concurrently prevent the aggregation of the metal atoms. This can be achieved with a substrate containing carbon, oxygen and nitrogen, due to strong binding of the metal atoms. This can be further enhanced with structural defects on the supports surface. Indeed, defect engineering can be exploited for the ingenious design of the coordination structures and hence manipulation of the catalytic activity. Notably, the obtained SAzymes can be readily dispersed in aqueous media; yet, a large size may impede the *in vivo* activity.^{35, 59}

ALD is another effective strategy to prepare SAzymes, which is based on a series of continuous self-limiting reactions occurring between the surface of an active precursor substance and an active substrate material.⁶⁰ The self-limiting characteristics promote the spontaneous formation of regular geometric structure of SAzymes, a unique feature to study the correlation between the materials structure and catalytic activity.⁶¹

Other methods, such as atom trapping⁶² and gas-phase migration⁶³, are also emerging. These allow the development of a diverse range of experimental methods for SAzyme preparation.

3. SAzyme Supports

Due to a high surface free energy, metal atoms tend to aggregate into nanoclusters or nanoparticles. It is therefore vital to select an appropriate supporting substrate to stabilize the individual metal atoms and prevent the aggregation. Within this context, two structural scaffolds have been used in the preparation of SAzymes, one carbon-based and the other noncarbon-based.⁶⁴

3.1 Carbon-based supports

Carbon-based supports mostly consist of graphene, graphene oxide, carbon nanotubes (CNTs), MOFs, and graphitic carbon nitride (g-C₃N₄). These supports are usually doped with N atoms, and can thus be used to form MN_x coordination moiety with the metal atoms (M = Fe, Cr, Zn, Mn, Cu, etc.).⁶⁵⁻⁶⁸ The exposed area of the active sites and the electron-transfer dynamics can be enhanced by the formidable metal-support covalent coordination.⁶⁹ For instance, Cheng et al.⁷⁰ designed a CNT-supported SAzyme (CNT/FeNC) consisting of FeN_x moieties, by using NaCl crystals as the removable templates (Figure 3). The CNT/FeNC SAzyme catalyzed the decomposition of H₂O₂ to hydroxyl radicals (\bullet OH) via the Fenton reaction. Such a POD-like activity was superior to those of Fe₃O₄ nanoparticles and other Fe-based nanozymes reported earlier. In another study, inspired by the actual shape of the heme cofactor of natural HRP, Lee et al.⁷¹ designed and synthesized FeN₄ single-site-embedded graphene (Fe-N-rGO), and observed a high enzymatic activity and selectivity, which was confirmed by density functional theory (DFT) calculations.

g-C₃N₄ is another effective supporting substrate for SAzymes, which exhibit preeminent POD-like activity in the generation of \bullet OH from H₂O₂ decomposition.^{72, 73} However, pristine g-C₃N₄ usually show a poor catalytic performance owing to the defects in the shape and internal structure.^{74, 75} Thus, a sharp-tip nanoneedle structure has been designed in order to alleviate the impediment of electron transfer by bulk g-C₃N₄ structure.⁷⁶ For instance, Fan et al.⁷⁷ fabricated a 3D branched g-C₃N₄ artificial enzyme through the ionothermal assay. The unique sharp-edge morphology formed by the modified synthetic process improved the crystallinity of g-C₃N₄, reduced charge-transfer resistance and accelerated H₂O₂ activation. The performance of g-C₃N₄ can also be enhanced by metal or non-metal doping. Jiang et al.⁷⁸ prepared g-C₃N₄ composed of sulfur-doped and sulfur-free active sites via liquid sulfur-mediation, where the doping of sulfur atoms led to a significant improvement of the catalytic performance. Likewise, the deposition of noble metal atoms (such as Pt, Pd, and Au) was found to induce localized surface plasmon resonance (SPR) which played a vital role in enhancing the catalytic activity.⁷⁹ In fact, defect engineering,⁸⁰ modification

tactics,⁸¹ and heterojunctions construction⁸² have been employed to improve the catalytic performance of g-C₃N₄.

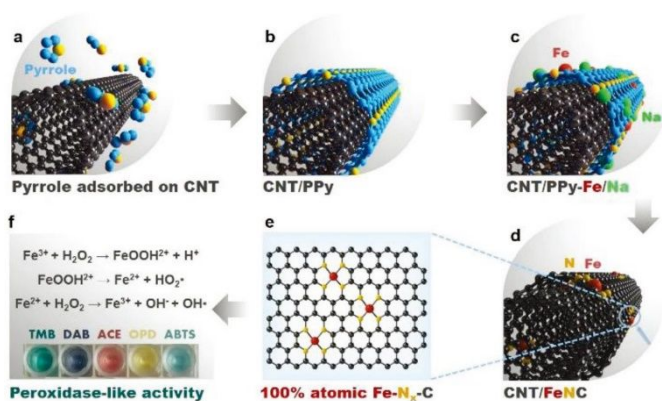


Figure 3. Schematic illustration of the synthesis and catalytic mechanism of Fe SAzymes using carbon nanotubes as a support substrate. (a) Adsorption of pyrrole molecules on CNT through π - π interactions. (b) Addition of ammonium peroxydisulfate induces pyrrole polymerization to obtain polypyrrole-coated CNT (CNT/PPy). (c) Adsorption of metal cations on CNT/PPy from the solution of $\text{Fe}(\text{NO}_3)_3$ and NaCl . (d) CNT/FeNC SAzyme obtained by pyrolysis of CNT/PPy with adsorbed metal ions in N_2 and then NH_3 . (e) Fe-N_x-C moieties in CNT/FeNC SAzyme. (f) POD activity of CNT/FeNC SAzyme in catalyzing the Fenton reaction to generate hydroxyl radicals ($\cdot\text{OH}$). This can be exploited for the oxidative degradation of 3,3',5,5'-tetramethylbenzidine (TMB, blue), di-azo-aminobenzene (DAB, gray), 3-amino-9-ethylcarbazole (AEC, red), o-phenylene diamine (OPD, yellow), and 2,2'-azino-bis (3-ethylbenzothiazoline-6-sulfonic acid) diammonium salt (ABTS, green). Reproduced with permission from ref. 70, copyright 2019, Wiley.

MOFs, another important class of carbon-based supports, are coordination polymers, which possess a porous and periodic network structure formed by the self-assembly of transition metal ions and organic ligands, and hence a large specific surface area and tuneable pore size. This enables intimate contact between the substrates and metal atoms and endows MOFs with artificially designed active sites and adjustable catalytic activity.^{83, 84} Indeed, MOF-based bioinspired nanomaterials with unique chemical activities, such as photodynamic, sonodynamic, and enzymelike activities, have found diverse biomedical applications, including tumor therapy, antibacterial therapy and antioxidant therapy (Figure 4). For instance, four pyrrolic nitrogen sites can form a plane-square structure, which is similar to a porphyrin motif. The center of the four sites acts as a solid trap to bind metal atoms and the surrounding N containing electron lone pairs as donors to coordinate with the target metal atoms.^{85, 86} Compared with metal-free porphyrins, metalloporphyrin-based organic linkers containing MN_x sites are formed when the two pyrrole protons (N-H) in the rigid macrocycles of porphyrin are replaced by metal ions, forming MN_x sites, which display enhanced catalytic activity due to the optimized electronic structure and accelerated electron transfer.⁸⁷ Therefore, MOFs with different structures and functions can be constructed through self-assembly between metal nodes and porphyrin-based organic linkages, such as tetrakis(4-carboxyphenyl)porphyrin (H₂TCP), 5,10,15,20-tetrakis(4-aminophenyl) porphyrin (TAPP), 5,10,15,20-tetrakis(4-pyridyl)porphyrin (H₂TPyP), (dicarboxyphenyl)porphyrin (BDCPP), and so on.⁸⁸ For example, manganese porphyrin-based MOFs (Mn-MOFs) have been found to exhibit unique SOD- and CAT-like activity, which can remove superoxide anion

free radicals, and have been used in tumor immunotherapy and nanovaccine fields.⁸⁹

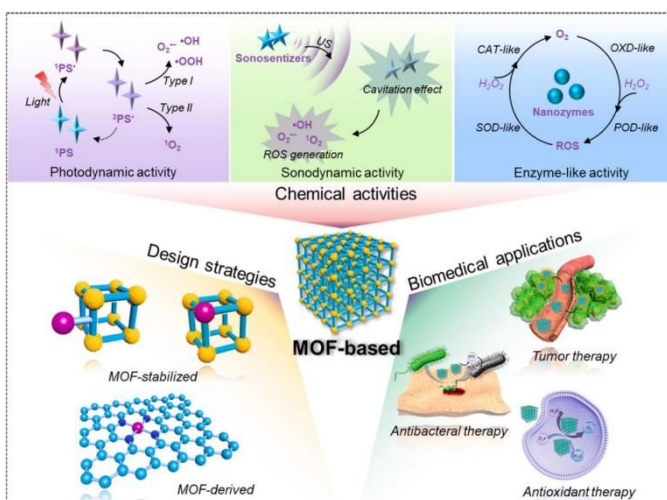


Figure 4. Design strategies and biomedical applications of MOF-based bioinspired nanomaterials with chemical activities. Reproduced with permission from ref. 84, copyright 2023, Elsevier.

Extensive research efforts have also been devoted to covalent organic framework (COFs).⁹⁰ The 2D structure of COFs furnishes a high-ordered arrangement and conjugated skeleton, along with a number of hollow sites for stable anchoring of transition-metal centers.⁹¹ For instance, Dong et al.⁹² prepared a 2D COF where the periodic organic building blocks were used to stabilize Pt single atoms while the heteroatom-rich (C, N, and O) pore walls afforded unique coordination environments to increase metal atom loading, leading to an increase of the active sites and catalytic activity. In another study,⁹³ Liu's group prepared a bipyridine-rich COF conjugated with Co single atoms via out-of-plane coordination. Note that in recent years, the COF-derived products are mostly used for photocatalytic applications,^{94, 95} with few as biological enzymes.⁹⁶ Further research is strongly desired.

3.2 Noncarbon-based supports

Noncarbon-based supports also attract great attention. Among these, transition metal oxide nanomaterials have become one of the most promising scaffolds.⁹⁷ The structural defects on the surface of metal oxides can act as binding sites for anchoring single metal atoms. Meanwhile, the distinctive crystal phases and rich electron configurations afford opportunities to form different coordination structures between the metal atoms and scaffolds. Indeed, a great quantity of transition metal oxide-based SAzymes have been prepared. Among these, TiO₂ has been used extensively as a support material, due to strong interactions with the metal atoms. Notably, Qiao's group prepared a Pt-TiO₂ SAC and noticed that metal-support interaction stemmed from the coordination environment rather than physical adsorption or sedimentation.⁹⁸ In fact, the metal oxide supports not only immobilize the dispersed metal atoms but also stabilize the geometric structure and modify the electronic structure, which can boost the catalytic performance.⁹⁹ Mechanistically, the lattice confinement in the internal structure of the supports acts as substitutable sites for the target metal atoms. In

contrast to the defect-stabilized structure, lattice confined sites are easier to be replaced.¹⁰⁰ Jiang's group synthesized a Pd/MnO₂ SAC with lattice-restricted structures, owing to the spatial constraint of Pt atoms by MnO₂, which spontaneously extracted surrounding lattice oxygen at room temperature with an ultralow energy barrier.¹⁰¹ The unique coordination environment formed by the metal atoms and metal oxide supports can significantly boost the catalytic activity towards a range of reactions, such as carbon monoxide oxidation reaction and decomposition reaction of hydrogen peroxide.

Transition metal sulfides have also served as effective supports. For instance, cobalt can be atomically dispersed onto a MoS₂ scaffold, and the resultant Co-MoS₂ SAzyme exhibits

metal-N δ bond that mimic the enzyme active centers.¹⁰³ Different valence states and electronic structures of the metal atoms give rise to different coordination configuration, and therefore the catalytic activity is closely related to the electron density, size¹⁰⁴ and number¹⁰⁵ of the metal centers. In fact, experimentally, the catalytic activity, selectivity and biological performance can be effectively regulated by manipulation of the metal species, coordination environment, heteroatomic doping and surface modification.³⁶ Below we will summarize the development of leading SAzymes within the context of the metal centers (Table1).

Table1. Summary of leading SAzymes with different metal centers

| Coordination structure | Synthetic method | Characterization | Enzyme-like activity | Biomedical applications | Ref. |
|------------------------|--|--|--------------------------------------|---|-------|
| Fe-N ₄ | pyrolysis | TEM, XRD | POD | biosensing | [107] |
| Fe ₅₅ -N-C | chemical coprecipitation and pyrolysis | SEM, TEM, HRTEM HAADF-STEM, XPS, XRD | POD | biosensing | [108] |
| Fe-N-C | wet-chemistry and high temperature calcination | SEM, TEM, HRTEM, STEM, XPS, XRD | POD | antibacterial therapy | [110] |
| Fe-N ₄ | pyrolysis and etching | TEM, STEM, XRD, XPS | GOx and HRP | biosensing | [111] |
| Fe-N ₅ | Hydrothermal synthesis | TEM, HAADF-STEM | OXD | biosensing and antibacterial therapy | [112] |
| Co-N-C | wet-chemistry | SEM, TEM, XRD | POD | biosensing | [114] |
| Co-N-C | hydrothermal and pyrolysis | TEM, HRTEM, STEM, XPS, XRD | OXD | biosensing | [115] |
| Co-N-C | coordination-pyrolysis-corrosion | TEM, HAADF-STEM, XANES, EXAFS | CAT | cancer therapy | [116] |
| Zn-N-C | pyrolysis | TEM, HAADF-STEM, XPS, XRD, EXAFS | POD | biosensing and antibacterial therapy | [118] |
| Pt-N-C | ionothermal method | SEM, TEM, HAADF-STEM, XPS | POD | H ₂ O ₂ detection and antibacterial therapy | [128] |
| Cu-N-C | wet-chemistry | TEM, XRD, XPS | POD, OXD | antibacterial therapy | [130] |
| Cu-N ₄ | electrochemical deposition | TEM, HAADF-STEM, EXAFS, XANES, XRD, XPS | ascorbate peroxidase-like (APX-like) | anti-oxidative damage | [27] |
| Ru-C ₆ | in situ one-pot multicomponent self-assembly | SEM, TEM, HAADF-STEM, XRD, XPS, NEXAFS | POD | cancer therapy | [164] |
| Mn-N-C | etching-adsorption-pyrolysis | TEM, HAADF-STEM, EXAFS, XANES, XAFS, XRD, XPS | CAT, OXD, POD | cancer therapy | [171] |
| Pd-N-C | "top-down" strategy | TEM, HRTEM, HAADF-STEM, EXAFS, XANES, XRD, XPS | POD, GSHOx-mimic | cancer therapy | [165] |

apparent POD-like activity.¹⁰² In summary, appropriate supports play a critical role in tuning the active sites, improving the catalytic performance and biological applications of SAzymes, which will be highlighted below.

4. Enzymatic Activity of SAzymes

A range of SAzymes have been prepared and used in diverse applications, in particular, biosensing and diagnostics. The metal center is an integral part of the SAzymes, which form M-N-C coordination moieties with surrounding N atoms through

Note: TEM, transmission electron microscopy; HRTEM, high-resolution transmission electron microscopy; HAADF-STEM, high-angle annular dark field-scanning transmission electron microscopy; SEM, scanning electron microscopy; XRD, X-ray diffraction; XPS, X-ray photoelectron spectroscopy; EXAFS, extended X-ray absorption fine structure; XANES, X-ray absorption near-edge spectroscopy.

4.1 Fe SAzymes

Fe-centered SAzymes, one of the most promising mimetic enzymes, have been extensively studied in recent decades, where the Fe-N-C coordination moiety serves as the active center due to geometric and electronic effects.¹⁰⁶ Among the numerous strategies of synthesis, controlled pyrolysis of zeolitic-imidazolite frameworks (e.g., ZIF-8) have been the leading method in recent years for the preparation of Fe SAzymes. For instance, Lin's group¹⁰⁷ prepared a FeN₄ SAzyme by pyrolysis of ZIF-8 and observed an unprecedented POD-like activity. Motivated by the structure of hemoglobin, Liu et al.¹⁰⁸ designed a precursor including hemin and ZIF-8 (Hemin@ZIF-8). During pyrolysis hemin served as the doping agent and effectively suppressed the aggregation of Fe atoms. Meanwhile, the larger Hemin would burst the cage of ZIF-8 and broke the confinement effect, creating a microporous multilayer structure and a high surface area. Experimentally, the group synthesized a series of Fe,N co-doped porous carbon, and observed that the POD-like activity in the TMB oxidation reaction varied with the initial feed of hemin, among which an optimal loading was identified.¹⁰⁹ Another noteworthy example is spherical mesoporous Fe-N-C SAzyme, which featured a large pore size (4.0 nm), high specific surface area (413.9 m² g⁻¹), uniform diameter (100 nm) and highly dispersed iron atoms.¹¹⁰ These characteristics facilitated mass transport and accessibility of the active sites, and hence boosted the POD-like activity.

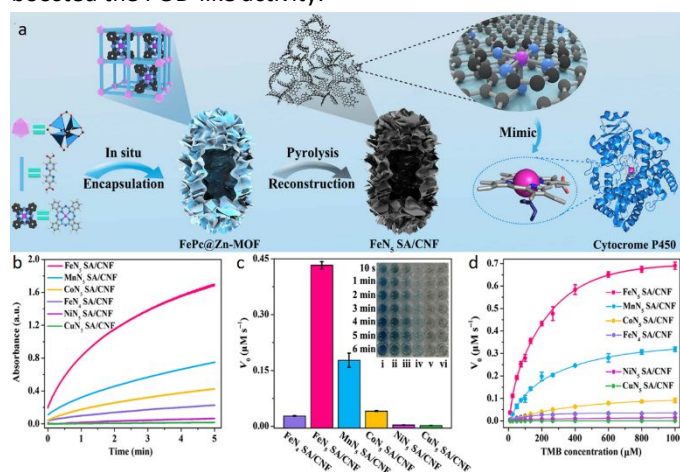


Figure 5. (a) Schematic formation process of carbon nanoframe-confined atomically dispersed Fe sites with axial N coordination for mimicking the active center of cytochrome P₄₅₀. (b) Comparison of the OXD-like activity of a series of nanozymes with a similar MN₅ structure (M = Co, Mn, Ni, and Cu), as manifested by the time-dependent absorbance of oxidized TMB (oxTMB) at 652 nm. (c) Histogram of the initial reaction rate (V_0) and (d) typical Michaelis-Menten curves in the presence of (i) FeN₅ SA/CNF, (ii) MnN₅ SA/CNF, (iii) CoN₅ SA/CNF, (iv) FeN₄ SA/CNF, (v) NiN₅ SA/CNF, and (vi) CuN₅ SA/CNF in air-saturated sodium acetate-acetic acid buffer. The inset to (c) is the photographs of the TMB solution in the presence of the various catalysts for up to 6 min. Reproduced with permission from ref. 112, copyright 2019, AAAS.

In a recent study,¹¹¹ we developed a platform for glucose sensing based on Fe SAzyme with a dual-signal readout mode based on fluorescence and electrochemistry. Experimentally, 3D porous N-doped carbon aerogels were used as the support matrix in which Fe single atoms were embedded to achieve uniform dispersion and maximize atomic utilization. Specifically, with SiO₂ nanoparticles as the structural templates, a gelatin-zinc hydrogel containing iron(II) phenanthroline (Fe(PM)₃²⁺) was exploited as the precursor and

subject to repeated freeze-drying at -20 °C. The resulting biomass hydrogel was then transformed into N-doped carbon aerogel anchored with Fe single atoms (NCAG/Fe) by pyrolysis and acid etching, which possessed a large surface area and rich mass transport channels and exhibited outstanding POD-like properties due to the formation of FeN₄ moieties. In fact, nonfluorescent OPD could be oxidized to fluorescent 2,3-diaminophenazine (DAP) by H₂O₂ generated by NCAG/Fe-catalyzed oxidation of glucose, and the fluorescence signal intensity varied with the glucose concentration; concurrently the oxidation of glucose also generated a significant electrochemical signal. Such a dual-signal detection platform could be exploited for the accurate and reliable detection of glucose even in clinical serum samples and artificial body fluids, as compared to commercial sensors.

Notably, Fe SAzymes may consist of not only FeN₄ but also FeN₅ coordination moieties, and the latter show a better catalytic activity, owing to the optimized coordination structure. For instance, inspired by the axial ligand-coordinated heme of cytochrome P₄₅₀, Huang et al.¹¹² rationally introduced a fifth nitrogen atom into the structure of FeN₄ to form axial coordination with the central iron atom. In the new assay, the organic nitrogen linkers were converted to pyridinic nitrogen at high temperature, which coordinated with the FeN₄ sites that were separated under the constraint of the carbon nanoframes (**Figure 5a**). The axial-coordination N atom of FeN₅ effectively activated O₂ and facilitated the cleavage of the O-O bond, behaving like natural oxide enzymes. At the same time, they systematically studied a series of nanozymes with a similar MN₅ structure (M = Co, Mn, Ni, and Cu), from which FeN₅ SA/CNF was found to exhibit the highest OXD-like activity, stability and biocompatibility (**Figure 5b-d**). Results from DFT calculations were highly consistent with the experimental conclusion. Taken together, these results show that the emergence of FeN₅ SAzymes provides a valuable reference in uncovering and understanding the enzyme-like mechanism and paves the way for ingenious formulation and appropriate applications of SAzymes.

4.2 Co SAzymes

As the heteromorphism of Fe₃O₄, the enzyme-like properties of Co₃O₄ nanoparticles have attracted wide attention, where the catalytic activity can be improved by changing the shape and increasing the specific surface area.¹¹³ For instance, Wang's group¹⁰² used the single-atom Co-MoS₂ nanozymes as a model, and combined experimental and theoretical studies to show that the Co centers and the MoS₂ supports involved different catalytic mechanisms: the former entailed an electron-transfer mechanism, while the latter was based on a Fenton-like reaction. The synergistic interactions between the Co single atoms and MoS₂ substrates greatly improved the POD-like activity of Co-MoS₂, which was successfully applied in the colorimetric and electrochemical sensing of hydrogen peroxide.

In another study,¹¹⁴ Co SAzymes were pyrolytically derived from ZIF-67 and a Cobalt salt template featuring unsaturated Co-porphyrin centers, and the resultant Co-PMCS SAzymes

exhibited excellent POD-like and other enzyme-like activities. This was then exploited for the colorimetric detection of a series of antioxidants by taking advantage of the color change of TMB oxidation by H_2O_2 catalyzed by the Co-PMCS SAzyme, where the color diminished in the presence of varied antioxidants. The sensor assay was demonstrated with 7 antioxidants, and exhibited a low detection limit, high accuracy, and good anti-interference capability. Sun's group exploited the inhibition of the OXD-like activity of Co-N-C SAzymes by thiols for the detection of biothiols (e.g., glutathione (GSH), cysteine (Cys)),¹¹⁵ as biothiols could bind to the Co centers, inhibit the adsorption of H_2O_2 , and thus block the oxidation process. Chen's group prepared a Co-SAs@NC SAzyme via a coordination-pyrolysis-corrosion process and observed CAT-like activity.¹¹⁶ In the tumor microenvironment, the SAzyme first acted as a CAT to decompose the endogenous H_2O_2 of tumor cells to O_2 , and then functioned as an OXD to catalyze the conversion of O_2 into highly cytotoxic $\text{O}_2^{\cdot-}$ radicals which led to apoptosis of the tumor cells.

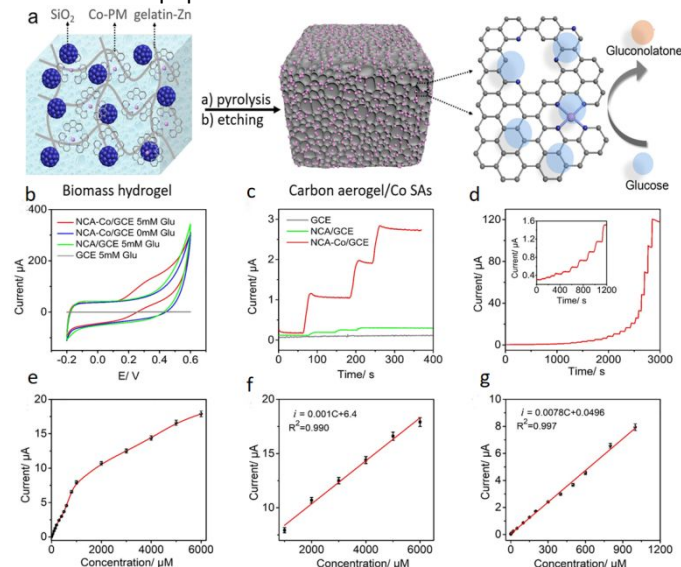


Figure 6. (a) Schematic of the preparation of NCA-Co aerogels derived from biomass hydrogels. (b) Cyclic voltammograms in 0.1 M NaOH at the scan rate of 50 mV s^{-1} of NCA-Co/GCE (GCE, glassy carbon electrode) in the absence and presence of 5 mM glucose, NCA/GCE, and bare GCE in the presence of 5 mM glucose. (c) Chronoamperometric profile of different modified electrodes at the applied potential of +0.3 V with the successive addition of 100 μM glucose into 0.1 M NaOH. (d) Chronoamperometric curve of the NCA-Co/GCE electrode upon the successive addition of glucose at various concentrations (0.5, 1, 2, 10, 20, 50, 100, 150, 200, 300, 400, 500, 600, 800, 1000, 2000, 3000, 4000, 5000, 6000 μM) into a 0.1 M NaOH solution at the applied potential of +0.3 V. Inset is the magnified segment for the glucose concentration range of 0.5 to 100 μM . (e) Current signals at different glucose concentrations and the corresponding linear correlation between the oxidation current increment and glucose concentration in the range of (f) 0.5–1000 μM and (g) 1000–6000 μM . Reproduced with permission from ref. 117, copyright 2022, Elsevier.

In a recent study,¹¹⁷ following the previous procedure of the preparation of NCA/Fe, we synthesized a Co SAzyme based on the similarly structured N-doped carbon aerogels. Again, the gelatin-zinc hydrogel was adopted as the precursor, into which were added a Co-PM complex and SiO_2 nanoparticles. The hydrogel was then pyrolytically converted into honeycomb carbon aerogels embedded with Co single atoms (NCA-Co) consisting of three active sites, CoN_4 in the basal plane, as well as CoN_4 and CoN_3 at the edge of the aerogel nanopores (Figure 6a). Theoretical calculations showed that the adsorption

energy of glucose at the different metal sites varied in the order of basal CoN_4 (−1.047 eV) < nanopore-edge CoN_3 (−0.811 eV) < nanopore-edge CoN_4 (−0.634 eV), suggesting the high catalytic activity of cobalt sites at the nanopore edges. When the NCA-Co nanozyme was used for electrochemical detection of glucose, good linearity was observed between the glucose concentration and current signal, due to the POD-like activity of the NCA-Co SAzyme (Figure 6b-g).

4.3 Zn SAzymes

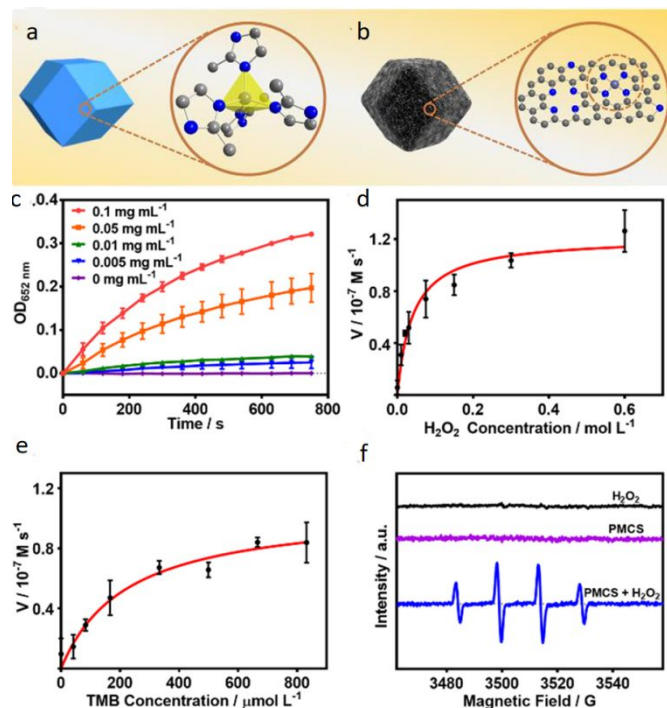


Figure 7. (a) Schematic illustrations of ZIF-8 with the ZnN₄ tetrahedral motif and (b) PMCS with the porphyrin-like structural model. (c) POD-like activity of PMCS at different concentrations in the catalytic oxidation of TMB. Steady-state kinetic assay of PMCS for (d) H_2O_2 and (e) TMB. (f) ESR spectra demonstrating $\cdot\text{OH}$ generation by H_2O_2 , PMCS, and PMCS + H_2O_2 . Reproduced with permission from ref. 118, copyright 2019, Wiley.

ZIFs are a kind of MOFs with a zeolite-like framework structure, which are produced by the reaction of metal ions, such as divalent Zn and Co, and imidazole or their derivative ligands in organic solvents, among which zinc-based ZIF-8 is the most commonly used ZIF and can be used to derive carbon nanocomposites containing atomically dispersed zinc atoms (Figure 7a).¹¹⁸ With the addition of target metal ions of a similar size of Zn^{2+} (e.g., Co^{2+} , Ni^{2+} , Fe^{2+} , etc.), the target metal ions can be homogeneously distributed into the metal nodes of the ZIF framework to form bimetallic ZIFs through coordination with the 2-methylimidazole linker. As the Zn species become evaporated at high temperatures, porous carbon is formed and embedded with the target metal ions. For ZIF-8 derived carbon (Figure 7b), the Zn-centered porphyrin-like moiety endows the sample (denoted as PMCS) with a POD-like activity, as manifested in the catalytic oxidation of TMB in the presence of H_2O_2 (Figure 7c-e). The unsaturated ZnN₄ coordination configuration acts as active sites and can catalyze the decomposition of H_2O_2 into hydroxyl radicals ($\cdot\text{OH}$), as confirmed in electron spin resonance (ESR)

measurements (Figure 7f). The optimal reaction conditions are similar to those for HRP, and the high activity can be retained within a wide range of pH and temperature. Xu et al.¹¹⁹ synthesized Mo/Zn dual-atom nanozymes supported on a macroscopic amphiphilic aerogel by pyrolysis of poly(vinyl alcohol) (PVA) and supramolecular coordination complexes.¹²⁰ The macroscopic dimension of the PVA substrate not only greatly enhanced the metal atom loading, but also stabilized the metal atoms. The Zn/Mo dual SAzyme showed a high metal content (1.5 and 7.3 wt% of Zn and Mo, respectively) without acid etching and with no structural collapse of the support, and synergistically led to a POD-like activity.

Of the Zn-based nanocomposites, the ZnN₄ moieties have been known to exhibit a high catalytic activity since the N atoms coordinating to the Zn center significantly lower the energy barrier and accelerate the electron-transfer kinetics. In fact, Zn SAzymes have shown potent antibacterial activity without external stimulation and toxicity to tissues and organs, in contrast to their nanoparticle forms.^{121, 122}

4.4 Pt SAzymes

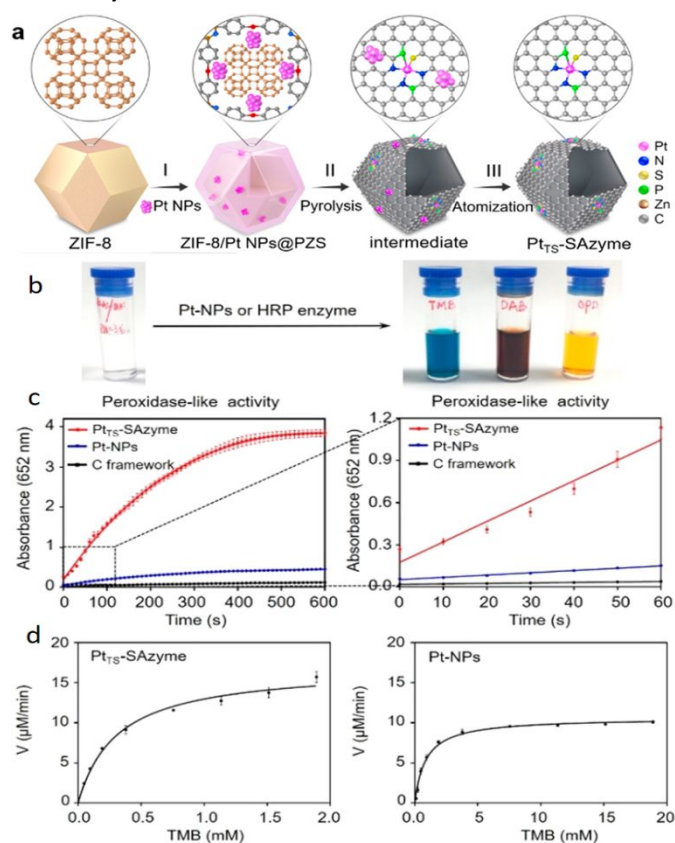


Figure 8. (a) Illustration of the preparation process of Pt-TS-SAzyme. (b) POD-like activity of Pt-based catalyzing the oxidation of POD substrates of TMB, DAB, and OPD to produce a color change. (c) (Left) Reaction-time curves of TMB oxidation catalyzed by Pt-TS-SAzyme, Pt-NPs nanozyme, or Pt-free inorganic C framework (NPS-HC); (Right) zoom in of the initial linear portion of the reaction-time curves. (d) Reaction kinetics of (Left) Pt-TS-SAzyme and (Right) Pt-NPs nanozyme. Reproduced with permission from ref. 127, copyright 2021, American Chemical Society.

Since the first report from Zhang' group that Pt/FeO_x SACs exhibited a high atom utilization and unexpected catalytic activity, Pt SAzymes have attracted widespread attention.¹²³ A host of Pt SACs have been produced and widely used in a

range of applications,¹²⁴ with CeO₂ being a unique support material.¹²⁵ For instance, Yan et al.¹²⁶ used Pt-CeO₂ SAzymes for the production of a new type of bandage for brain trauma. In vitro and in vivo experiments disclosed that the nanozyme-based bandage afforded sustained multienzyme activity (including POD-, CAT-, SOD-, and GPx-like activities), nontoxicity and excellent durability. The bandage significantly improved wound healing and reduced inflammation, which set a precedent for the noninvasive therapy of SAzymes.

Liang et al. developed a practical strategy for engineering high-performance nanozymes by reversing the thermal sintering process, which atomized platinum nanoparticles into single atoms within a carbon matrix derived from ZIF-8 (Figure 8a).¹²⁷ The P and S dopants not only promoted the atomization of Pt nanoparticles to Pt-TS-SAzyme, but also facilitated the formation of Pt₁N₃PS active moieties due to electron donation of the P dopants and electron acceptance of the N and S dopants. The resultant Pt-TS SAzyme was found to exhibit a remarkable POD-like activity by catalyzing the oxidation of POD substrates (e.g., TMB, DAB, and OPD) to produce a color change (Figure 8b). After thermal atomization of Pt nanoparticles into Pt single atoms, the POD-like catalytic activity and initial reaction velocity of Pt-TS-SAzyme were significantly higher than those of Pt nanoparticles or Pt-free N, P and S co-doped hollow carbon polyhedron (NPS-HC) (Figure 8c-d). Pt SAzymes have also been prepared with Pt single atoms supported on g-C₃N₄ via a wet chemistry strategy with alkali metal ions-intercalated g-C₃N₄ (g-C₃N₄-K) and a platinum salt precursor. The resulting SA-Pt/g-C₃N₄-K SAzyme remarkably enhanced the generation of •OH radicals by reducing the desorption energy of the intermediate state of OH* from the active site during H₂O₂ activation.¹²⁸ This opens up a new way in the antibacterial application of Pt SAzymes.

4.5 Other SAzymes

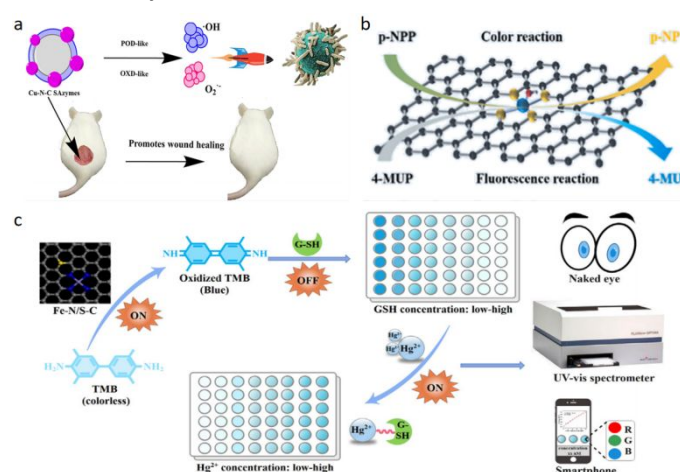


Figure 9. (a) Schematic diagram of the antibacterial activity of Cu-N-C SAzymes with intrinsic POD- and OXD-like activity. Reproduced with permission from ref. 130, copyright 2022, American Chemical Society. (b) Schematic diagram of the catalytic mechanism of Ce-N-C SAzyme with PPA-like activity for the rapid and sensitive detection of aluminum ions through color change and fluorescence signal generation during the catalytic process. Reproduced with permission from ref. 131, copyright 2022, Elsevier. (c) Schematic diagram of a colorimetric sensor based on Fe-N/S-C SAzymes for simultaneous multimode detection of GSH and Hg²⁺. Reproduced with permission from ref. 137, copyright 2022, Elsevier.

Other metals have also been used to prepare SAzymes. Among the metals with bactericidal effect, copper can effectively inhibit the growth of various harmful bacteria, viruses and microorganisms in water (such as algae). However, as a heavy metal, the biological applications of copper and its compounds have remained limited due to metal toxicity.¹²⁹ The metal leaching effects can be minimized with Cu SAzymes. Zhu et al. observed that Cu SAzymes with Cu-N-C moieties exhibited intrinsic POD- and OXD-like activity to catalyze the generation of $\bullet\text{OH}$ and $\text{O}_2^{\bullet-}$ from H_2O_2 and O_2 , respectively.¹³⁰ The produced ROS displayed a significant activity towards the inhibition of bacterial growth. As the antibacterial activity of the Cu SAzymes was significantly superior to vancomycin, a common antibacterial drug (**Figure 9a**), it is anticipated that Cu SAzymes will play a critical role in the development of new antibacterial agents and new antimicrobial strategies.

Song et al. observed an excellent phosphatase-like (PPA-like) activity with Ce-N-C SAzymes, which effectively catalyzed the dephosphorylation process of inorganic phosphate.¹³¹ Notably, as Al^{3+} could form Al-O bond via specific binding with O atom and inhibit the PPA-like activity (**Figure 9b**), a fast, low cost, portable, and efficient fluorescent liquid-phase sensor can be constructed for the sensitive detection of Al^{3+} .

Some other metals, such as Ru, Co, Au, and Se, have also been used as the active centers for SAzyme.¹³² They are usually synthesized by wet chemistry and high-temperature pyrolysis. Notably, two different metal atoms can be combined to construct dual-atom structures, where the synergistic effects can be exploited for the manipulation of the electronic structure of the metal centers.¹³³ In earlier studies, these materials were mainly used as electrode catalysts for electrochemical energy technologies. In recent years, they have shown great potential in biomedical applications, such as tumor therapy and biosensing, with the continuous optimization of the structures and emergence of a variety of enzyme-like activities,¹³⁴ as demonstrated below in section 4.6.

4.6 Nonmetal dopants

For SAzymes, the M-N-C active moiety can be further engineered with the introduction of additional heteroatom dopants, such as O, S, and P, by taking advantage of their different electronegativity to manipulate the electronic property of the metal centers.¹³⁵ For instance, in comparison to the FeN_4 SAzyme and Fe_3O_4 nanozyme, FeN_3P SAzyme by P doping into the Fe-N-C SAC exhibited markedly enhanced POD-like activity, as manifested in the colorimetric reaction of hydrogen peroxide and TMB.¹³⁶ DFT calculations showed that the adsorption energy of hydrogen peroxide was lowered to -0.40 eV on FeN_3P , as compared to -1.24 and -0.60 eV on $\text{Fe}_3\text{O}_4(111)$ and FeN_4 , respectively, consistent with the enhanced kinetics of the dissociation of hydrogen peroxide into two surface OH species ($\text{H}_2\text{O}_2 \rightarrow 2\text{OH}$). Subsequently, in the FeN_3P SAzyme, FeN_4 SAzyme and $\text{Fe}_3\text{O}_4(111)$ nanozyme, the two surface OH species reacted with each other to form surface O and H_2O molecule ($2\text{OH} \rightarrow \text{O} + \text{H}_2\text{O}$) with an energy barrier of 0.49, 1.05 and 1.51 eV, respectively, which indicated that this process was most easily carried out on the surface of

FeN_3P SAzyme. However, since the H_2O molecules were still adsorbed on the surface of the nanozyme, this could inhibit the catalytic process. A thermodynamic investigation was then conducted to examine the desorption of water molecules. The results showed that the desorption energy of water molecules was relatively low on the surface of all the three nanozymes under neutral conditions. In acidic media, the reaction potential energy of the transformation of OH species into H_2O on FeN_4 SAzyme was increased to 2.84 eV, suggesting that OH would be stuck to the Fe centers and impede the catalytic process; by contrast, OH could be instantaneously converted into H_2O on $\text{Fe}_3\text{O}_4(111)$, due to an ultralow reaction potential energy of 0.11 eV, which also led to failure of the catalytic process. Yet, the reaction potential energy of this process on FeN_3P SAzyme was almost independent of solution pH, indicating that the surface OH species could be successfully converted into H_2O . The desorption of H_2O can also occur easily due to a low barrier on the three nanozymes. In summary, the proposed reaction pathway demonstrated an enhanced catalytic activity of FeN_3P SAzyme due to synergistic effects of the P dopants through the precise coordination to the metal centers. Similarly, Li et al.¹³⁷ introduced S dopants into Fe-N-C SAzyme, which not only manipulated the geometric configuration and electronic structure of the metal centers, but also reduced the formation of inactive Fe carbide, and facilitated the formation of a porous carbon structure with a high specific surface area. The resulting Fe-N/S-C SAzyme exhibited enhanced OXD-mimicking activity due to the auxiliary regulation of the S atoms, as compared to the Fe-N-C counterparts (**Figure 9c**).

Doping of polynary metals has also been employed to construct SAzymes with a high density of activity sites, where the addition of multiple metals can form active sites and regulate the electronic structure through the interactions between the metals centers.¹³⁸ Therefore, the binding energy of reactants, intermediates, and products can be modulated for an optimal catalytic performance. In a recent study,¹³⁹ a Fe-Bi bimetallic SAzyme (Fe/Bi-NC) was prepared by using Fe-doped Bi-MOF as the precursor, and consisted of Fe- N_4 and Bi- N_4 dual-sites. The role of Fe was not only to generate active sites, but also to expand the distance of neighboring Bi atoms and prevent their aggregation. Meanwhile, PVP surfactants were added to prevent the interlayer accumulation of the MOF precursor through chemical adsorption. During pyrolysis the precursor was transformed into thin-sheet Fe/Bi-NC, a unique structure conducive to the formation of single-atom sites. Experimental studies and DFT calculations confirmed the positive synergistic effect between the FeN_4 and BiN_4 sites, which markedly enhanced the OXD-like activity. Yet, an Fe content over 4% actually diminished the enzymatic activity. Therefore, accurate regulation of the contents of constituent atoms is critical for attaining ideal bimetallic SAzymes. In another study, Au-Ni/g- C_3N_4 SAzymes were produced with g- C_3N_4 nanosheets doped with Au-Ni bimetallic nanoparticles,¹⁴⁰ which exhibited apparent POD-like activity and could be used for the colorimetric detection of glucose. In enzyme kinetics measurements, the K_m values were found to be lower with the

bimetal SAzymes than those of their monometallic counterparts, indicating enhanced affinity of the Au-Ni/g-C₃N₄ nanocomposite toward the substrates. In fact, the enhanced catalytic activity was attributed to the synergistic effects between the Au and Ni atoms. Due to a clear difference of the ionization potential between Au and Ni (9.22 eV and 7.63 eV), electron transfer occurred from Ni to Au, resulting in an increase in the charge density of Au, such that both Au and Ni could act as active sites for the POD-like activity. This bimetallic synergistic effect has also been previously reported in the literature.¹⁴¹

In summary, one can see that metal centers are the active sites that dictate the catalytic activity of SAzymes, due to the formation of unique M-N-C coordination structures.¹⁰³ For instance, among the Fe-based SAzymes, the FeN₃ moiety is known to exhibit a strong OXD-like catalytic activity because O₂ molecules adsorb readily onto the FeN₃ centers via a side-on configuration, which is the first step in the OXD-like reaction and plays an important role in the subsequent steps.¹⁴² FeN₄ SAzymes, however, usually exhibit excellent POD-like activity, because the FeN₄ active sites mimics the porphyrin iron cofactor structures (Fe atoms coordinated to four nitrogen atoms in the plane of the porphyrin ring) of natural HRP.³⁶ For FeN₅ SAzymes, the electronic structure of the Fe centers is optimized, due to the addition of the axial ligand through the nitrogen atom, which facilitates the electron-transfer kinetics and leads to a better OXD- and POD-like activity than that of FeN₃ and FeN₄.⁵⁵

Similarly, with a zinc-centered porphyrin-like structure, Zn-based SAzymes also display outstanding POD-like activity. The unsaturated-coordination ZnN₄ centers can catalyze the decomposition of H₂O₂ into •OH, which is similar to the catalytic pathway of HRP.¹⁴³ Cu-based SAzymes not only exhibit OXD- and POD-like activity but also mimic polyphenol oxidase (e.g., tyrosinase, catechol oxidase, and laccase), where the active sites all feature coupled multinuclear Cu(II) centers and can oxidize important biological substrates (e.g., polyphenols and polyamines) and directly activate oxygen.¹⁴⁴

Notably, these enzymatic activities are sensitively dependent on solution pH. Under different pH conditions with different metal centers, H₂O₂ can be decomposed into different forms. Specifically, SAzymes typically exhibit POD-like activity at low pH and CAT-like activity at high pH.¹⁴⁵ The number of coordinating nitrogen can also impact the catalytic activity. For example, when the number (*x*) of coordinating N in CoN_{*x*} decreases from 4 to 2, Co SAzymes show an enhanced activity towards oxygen reduction reaction,¹⁴⁶ while FeN₅ SAzymes display a better OXD- and POD-like activity than both FeN₄ and FeN₃.

Therefore, to improve and optimize the catalytic performance of SAzymes, the elemental composition, metal coordination configuration, metal loading and supports interactions need to be systematically varied and carefully examined,¹⁰⁴ as they affect the geometric configuration and electronic structure of the metal centers, resulting in different catalytic activity and selectivity. This is of particular importance for SAzymes that possess multi-enzyme activity

and find diverse applications in antibacterial, cancer therapy, and cell protection.¹⁴⁷

5. Biological and Medical Applications

5.1 Biosensing

Due to the low cost, high efficiency, high sensitivity and great stability, SAzymes have been successfully utilized in the construction of a variety of biosensors based on colorimetric, electrochemical and fluorescence platforms.¹⁴⁸ Most colorimetric biosensors are based on the TMB redox chemistry, as TMB can be oxidized to a blue product (oxTMB) catalyzed by the POD-like activity of SAzymes, which can be readily detected with an absorption peak at 652 nm, and the concentration of the target analyte can be determined from the absorbance.¹⁴⁹ For instance, Zhou et al.¹⁵⁰ fabricated an Fe SAzyme by an isolation-pyrolysis procedure which displayed POD-like activity and catalyzed the oxidation of TMB in the presence of H₂O₂ generated from the oxidation of galactose with galactose oxidase (Gal Ox) (**Figure 10a**). The colorimetric sensor exhibited a good linear relationship between the optical absorbance and galactose concentration, with a good minimum detection limit, which paved the way for a rapid and economical detection of galactose and diagnosis of galactosemia. Similarly, in a Bi SAzyme anchored onto Au hydrogels (BiSA@Au),¹⁵¹ the Bi atoms and the unique porous nanowire networks of the hydrogels greatly improved the catalytic activity by decreasing the potential barriers for the decomposition of H₂O₂. With the immobilization of GOx on the surface of the BiSA@Au nanozyme, the oxidation of TMB could be exploited for the accurate and sensitive colorimetric detection of glucose in clinical samples. In another study with FeN₃/PtN₄ dual-atom SAzymes,¹⁵² a colorimetric sensing platform was obtained for the quantization of dopamine whereby the POD-like activity of FeN₃/PtN₄ was utilized to catalyze the oxidation of TMB by H₂O₂ to generate blue oxTMB, and then the addition of dopamine reduced oxTMB back to colorless TMB (**Figure 10b**). Similarly, Feng et al. synthesized B-doped Zn-N-C (ZnBNC) SAzymes for the colorimetric detection of p-phenylenediamine (PPD), a reductive carcinogen,¹⁵³ which reduced blue oxTMB to colorless TMB, with a linear decrease of the absorbance with PPD concentration (**Figure 10c**).

Notably, the oxidation of TMB can be inhibited by a range of small-molecule compounds that are effective indicators of human health, such as uric acid, dopamine, norepinephrine and ascorbic acid. This unique chemistry can be exploited for the development of biosensors for their indirect detection.¹¹⁴ For instance, Wu et al. prepared an Fe SAzyme with a high OXD-like activity at pH 3.0, and the activity could be effectively inhibited by 4-acetamidophenol (AMP) via a reversible mixed-inhibition mechanism.¹⁵⁴ This unique property could be exploited for the detection of AMP.

In electrochemical biosensing, Hu et al.¹⁵⁵ prepared an A-Co-NG SAzyme with Co atomically dispersed into N-doped graphene for electrochemical detection of uric acid by

measuring the change of the current signals involved in the oxidation of uric acid molecules. Liu et al.¹⁵⁶ optimized the Co-N-C structure of a Co SAzyme by embedding Co atoms into a reduced graphene oxide aerogel (rGA) forming a three-dimensional layered electrochemical electrode, which exhibited a high electrocatalytic performance in the in-situ detection of H₂O₂, uric acid and dopamine. By monitoring the current response of Co-N-C, rGA and Co-N-C/rGA on a GCE under different experimental parameters, it was found that Co-N-C/rGA exhibited the best catalytic performance among the series (**Figure 10d**).

Notably, POD-mimicking nanozymes require an acidic medium to exhibit the enzymatic activity, while near-neutral pH is the optimal condition for GOx. The cumbersome steps of switching pH during the sensing operation bring tremendous obstacles to the cascade reaction of the two enzymes. To mitigate these issues, a foldable paper microfluidic device has been rationally designed which is divided into two parts at acidic and neutral pH for the Fe SAzymes and GOx, respectively (**Figure 10e(i)**).¹⁵⁷ Experimentally, glucose is oxidized by GOx under neutral pH generating H₂O₂, which then migrates to the other compartment by folding the paper device producing a colorimetric signal under acidic pH (**Figure 10e(ii)**). The unique technology breaks the pH restriction of cascade reactions and may serve as an innovative portable integrated microdevice for rapid detection of glucose, a key step in the further development of point-of-care testing (POCT) (**Figure 10e(iii)**). In fact, a range of biosensors are being developed within the context of miniaturization, integration and wearability. The devices are portable, exhibit a fast detection speed, and can be integrated with artificial intelligence and informational technology for remote, real-time monitoring. Nevertheless, there are not many examples of SAzymes used in these applications yet. The construction of stable point-of-care testing (POCT) devices with SAzymes instead of natural enzymes is anticipated to greatly extend the sensor lifetime. Improving the stretchability of SAzymes through rational design to build wearable biosensing devices will also create an emerging pathway.¹⁵⁸

Furthermore, fluorescence-based biosensors have also been fabricated with SAzymes.¹⁵⁹ For instance, Wang et al.¹⁶⁰ utilized the POD-like activity of Fe SAzymes to catalyze the oxidation of nonfluorescent OPD to fluorescent DAP, with a maximum fluorescence emission peak at 566 nm. The generated DAP efficiently quenched the fluorescence emission of polyvinylpyrrolidone-protected copper nanoclusters (PVP-CuNCs) at 438 nm; yet this could be blocked by thiocholine derived from acetylthiocholine by acetylcholinesterase (AChE). Therefore, the ratio of the fluorescence emission at 566 and 438 nm (F_{566}/F_{438}) could be exploited for the quantification of the AChE activity (**Figure 10f**).

In addition to the above-mentioned biosensors, nanozyme-based immunosensors have also been reported. In a typical sandwich-type immunosensor, the target (antigen) first binds to the corresponding specific antibody, followed by the neuraminidase (NANase)-linked antibody, which then binds to the recognized antigen, thus forming a sandwich structure. For

SAzyme-based immunosensors, the optimized electronic structure can lead to a high catalytic activity. The introduction of SAzymes catalyzes some chromogenic reactions, which to some extent compensates for the lack of sensitivity of colorimetric analysis, while maintaining a good activity after prolonged storage within a wide range of pH and temperature.¹⁶¹

Furthermore, the accurate detection of DNA usually requires a combination of signal amplification strategies by, for instance, nanozymes. However, the use of SAzymes for this purpose has been relatively rare. It can be envisaged that when a DNA probe is modified with SAzymes that can catalyze the chromogenic reaction of the relevant chromogenic substrate, precise detection of DNA can be achieved in conjunction with a signal amplification strategy.¹⁶²

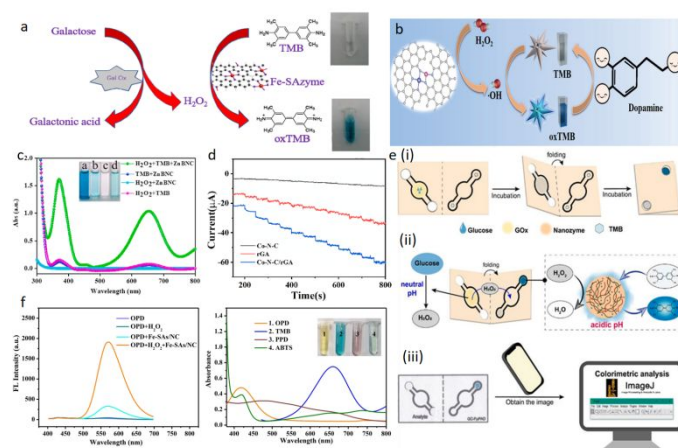


Figure 10. (a) Schematic illustration of the colorimetric assay for galactose detection by an Fe SAzyme. Reproduced with permission from ref. 150, copyright 2020, Elsevier. (b) Schematic illustration of dopamine determination by Fe₃/PtN₄ dual-site SAzymes. Reproduced with permission from ref. 152, copyright 2022, Springer. (c) UV-vis spectra of ZnBNC, ZnNC and H₃BO₃-ZnNC in the H₂O₂/TMB solution. Inset is the photograph of the various solutions. Reproduced with permission from ref. 153, copyright 2020, Elsevier. (d) Amperometric response of Co-N-C, rGA and Co-N-C/rGA on a GCE with the addition of 100 μM H₂O₂ in 0.01 M PBS (pH 7.4). Reproduced with permission from ref. 156, copyright 2020, Elsevier. (e) Schematic illustration of the colorimetric detection of glucose via PGA-Fe/CS NPs-incorporated foldable paper microfluidic device (PGA-Fe/CS@FμPAD). (i) Glucose detection procedure, (ii) cascade reaction incorporating glucose oxidation under neutral pH and H₂O₂ reduction with TMB oxidation under acidic pH, and (iii) on-site quantification via an image acquired with a smartphone. Reproduced with permission from ref. 157, copyright 2023, Elsevier. (f) (Left) Fluorescence emission spectra of OPD, OPD/H₂O₂, OPD/Fe-SAs/NC, and OPD/H₂O₂/Fe-SAs/NC, and (Right) UV-vis absorption spectra of H₂O₂/Fe-SAs/NC with the substrates of OPD, TMB, PPD and ABTS. Inset is the photograph of the varied solutions. Reproduced with permission from ref. 159, copyright 2020, Elsevier.

5.2 Cancer diagnosis and therapy

SAzymes featuring various enzyme-like activities have also been creatively introduced to assist the diagnosis and treatment of cancers, which is efficient, non-toxic, biocompatible, and non-invasive (**Figure 11**).^{163, 164} Ferroptosis is a cell death mechanism discovered in 2012. It is caused by the accumulation of iron-dependent lipid peroxidation (LPO), which induces lethal disruption of the cell membrane structure. Glutathione peroxidase 4 (GPx-4) can reduce the production of LPO by taking GSH as a cofactor, but glutathione oxidase (GSHOx) will promote the conversion of GSH to glutathione disulfide (GSSG), resulting in the deactivation of GPx-4 and thus increasing the accumulation of LPO. In 2021, Lin's group reported an innovative strategy of mild photothermal therapy (PTT) based on Pd SAzymes to promote

the treatment of ferroptosis.¹⁶⁵ The Pd SAzyme showed POD- and GSHOx-like activities and photothermal conversion performance, which could lead to the up-regulation of LPO and ROS. The accumulation of LPO and ROS provided a powerful way to split heat shock proteins (HSPs) which could repair cell damages caused by heat, making Pd SAzyme-mediated mild PTT possible.

In 2022, considering the effects of hyperthermia on the activity of SAzymes and the damage of cell tissue, Liu's group used $\text{Bi}_2\text{Fe}_4\text{O}_9$ nanosheets as an enzyme mimic by low-temperature activation (4 – 37 °C), which featured a wider safety window than those treated at higher temperatures (37 – 42 °C). The cold-activated SAzyme displayed GSHOx- and POD-like activity and mediated the antitumor treatment.¹⁶⁶ Notably, the GSHOx-like activity of the $\text{Bi}_2\text{Fe}_4\text{O}_9$ SAzyme could only be activated at low temperatures, whereas the POD-like activity of $\text{Bi}_2\text{Fe}_4\text{O}_9$ SAzyme in acidic media and the CAT-mimic activity in neutral and alkaline conditions were unaffected by temperature changes. Therefore, the GSHOx-like activity activated at low temperatures promoted the oxidation of GSH to generate H_2O_2 . Then intrinsic H_2O_2 together with the H_2O_2 generated from GSH oxidation was decomposed by POD-like $\text{Bi}_2\text{Fe}_4\text{O}_9$ SAzymes. When the GSHOx-like activity was turned off by an interventional device (e.g., a smart phone), the enzyme activity could be remotely and precisely modulated, so as to eliminate excessive ROS through CAT-like activity and minimize damage to normal tissues. Similarly, Wu's group observed that a Ni SAzyme doped with sulfur and nitrogen via an anion exchange method showed better POD- and GSHOx-like activity than the undoped counterparts and could effectively inhibit the growth of tumor cells without toxicity (Figure 11a).¹⁶⁷

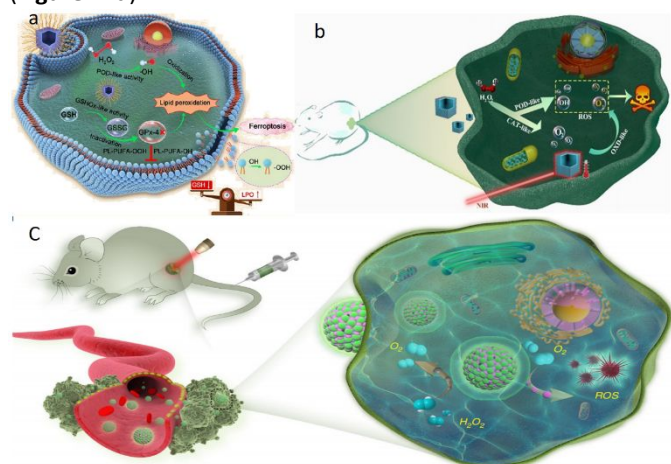


Figure 11. (a) Illustration of inhibiting tumor cell growth by inducing iron ferroptosis. Sulfurized S-N/Ni PSAE exhibits higher GSHOx-like activity than nitrogen-monodoped N/Ni PSAE for depleting intracellular GSH, resulting in the inactivation of GPX-4. Moreover, S-N/Ni PSAE with superior POD-like activity converts endogenous H_2O_2 into highly toxic $\bullet\text{OH}$, causing LPO via oxidizing PUFAs. Reproduced with permission from ref. 167, copyright 2023, American Chemical Society. (b) Illustration of manganese-based single-atom enzyme for tumor therapy utilizing the synergetic catalytic and photothermal therapy. Reproduced with permission from ref. 171, copyright 2021, Wiley. (c) Scheme of continuously catalytic oxygen generation and ROS production for enhanced tumor photodynamic therapy by OxgeMCC-r SAzyme. Reproduced with permission from ref. 164, copyright 2020, Springer Nature.

As the tumor microenvironment features insufficient oxygen supply and excessive ROS (such as H_2O_2),¹⁶⁸ one can take advantage of the unique activity of SAzymes to catalyze the

decomposition of H_2O_2 to cytotoxic hydroxyl radicals ($\bullet\text{OH}$) and locally kill the tumor cells. This was indeed demonstrated recently by He et al. with a Pd SAzyme based on phenolic carbon quantum dot (DA-CQD@Pd).¹⁶⁹ Meanwhile, SAzymes can catalyze free-radical polymerization to form immune adjuvant CpG oligodeoxynucleotides (ODN), which can initiate catalytic immunotherapy to achieve localized immunomodulation and prevent tumor metastasis. Liu's group prepared an Fe SAzyme containing FeN_5 moieties embedded within N-rich carbon via a melamine-mediated two-step pyrolysis strategy,⁵⁵ where the FeN_5 active sites catalyzed the decomposition of H_2O_2 to $\bullet\text{OH}$. Feng's group integrated Au nanoparticles into the pores of a dendritic mesoporous Fe SAzyme,¹⁷⁰ where the Au nanoparticles interacted with glucose to generate gluconic acid and H_2O_2 in a nanozyme-like manner, and H_2O_2 was further decomposed into ROS due to the POD-like activity of the Fe SAzyme. This kind of GOD-like activity can cut off the energy supply of the tumor cells, and in combination with photothermal agents (PTAs), achieve photothermal treatment of tumors at low temperatures.

Apart from the POD-like activity, many SAzymes possess multienzyme properties and can initiate cascade enzymatic reactions and enhance the therapeutic efficacy. Zhu et al. utilized hollow ZIF as a precursor to prepare a PEGylated manganese-based SAzyme (Mn/PSAE), which catalyzed the conversion of cellular H_2O_2 to $\bullet\text{OH}$ by the POD-like activity, as well as promoted the production of O_2 from H_2O_2 and the conversion of O_2 to $\text{O}_2^{\bullet-}$ via OXD-like activity.¹⁷¹ The amorphous carbon substrate materials could enhance the PTT effect. In short, the enzyme cascade reactions initiated by SAzymes with multienzyme catalytic properties facilitate the continuous redox reaction of cells and the accumulation of cytotoxic ROS, which is a favorable and implementable pathway to enhance the anti-tumor effect (Figure 11b).

Despite such breakthroughs in SAzyme-based tumor therapy, there remains much room to improve the specificity. Studies have shown that the combination of nanomotor and near-infrared (NIR) technology can enhance adhesion of SAzymes to the cancer cell membrane and deepen penetration into the tumor.¹⁷² Another desirable route is to combine chemodynamic therapy,¹⁷³ sonodynamic therapy¹⁷⁴ and photothermodynamic therapy¹⁷⁵ to improve targeting. One can envision that precise drug administration can be achieved when drugs are loaded onto the SAzymes for targeted transport to the cancer sites.¹⁷⁶ In conclusion, targeted tumor therapy has remained a key clinical challenge, and SAzymes have emerged as a unique platform, which demands further and more thorough studies.

5.3 Antibacterial and antiviral activity

Bacterial infection is a grave threat to human health, which is compounded by the emergence of drug-resistant bacteria. ROS can act as powerful weapons against pathogen invasion by disintegrating the structure of biofilms, while avoiding the generation of drug-resistant strains due to effective damages of bacterial cells.^{177, 178} SAzymes possess unique advantages as compared to traditional antibacterial agents, such as high

efficiency, low cost, good biocompatibility, non-cytotoxicity and adjustable enzyme activity, where the bactericidal mechanism is primarily based on in vivo decomposition of hydrogen peroxide or oxygen to ROS.¹⁷⁹

Previous reports have shown that Cu SAzyme exhibited excellent antibacterial activity. Zhao et al. prepared a highly accessible Cu SAC supported on biocompatible N-doped mesoporous carbon nanospheres via an emulsion-template method.¹⁸⁰ The ultra-large pore size and small particle size of the mesoporous carbon nanospheres boosted the efficient conversion of O₂ to O₂^{•−}, resulting in the damage of bacterial cell membrane and the splitting of the bacterial body. Wang et al. synthesized N-doped porous carbon-supported Cu SAzymes (Cu SAs/NPC) by a pyrolysis-etching-adsorption-pyrolysis (PEAP) strategy.¹⁸¹ The Cu SAzymes possessed prominent POD-like activity in catalyzing the decomposition of H₂O₂ to •OH and GSH peroxidase (GSH-Px)-like activity to deplete GSH, and consequently a nearly 100% antibacterial efficacy against the two most common pathogenic bacteria, *Escherichia coli* (*E. coli*) and methicillin-resistant *Staphylococcus aureus* (*S. aureus*) through the synergistic effect of PTT (Figure 12a). Meng et al. utilized a unique support consisting of a nanodiamond core and curved graphene shells (ND@G) that was decorated with abundant defects to anchor Cu metal atoms, resulting in atomically dispersed and fully exposed Cu₃ clusters on the ND@G surface (Figure 12b).¹⁸² This structure significantly enhanced the OXD-like activity in the dissociation of O₂ into •OH to kill bacteria.

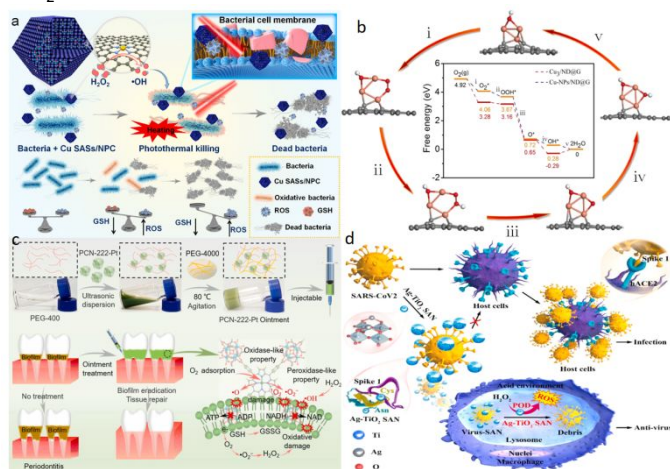


Figure 12. (a) Cu SAs/NPC with GSH-depleting performance for photothermal-catalytic therapy against bacterial. Cu SAs/NPC as GSH-like mimetic enzyme and HRP-like nanozyme for eradicating *E. coli* and *MRSA* in vitro. Reproduced with permission from ref. 181, copyright 2021, Elsevier. (b) Theoretical investigation of OXD-like activity over Cu₃-NPs/ND@G and Cu₃/ND@G. The optimized adsorption configurations of various intermediates along the oxidase-like reaction path on Cu₃/ND@G and the free energy diagram for the oxidase-like mechanism on Cu₃/ND@G and Cu₃-NPs/ND@G. The gray, brown, red and white balls represent C, Cu, O, and H atoms, respectively. Reproduced with permission from ref. 182, copyright 2022, Elsevier. (c) Preparation of the injectable HNTM-Pt ointment with enzyme-like catalytic activities and the treatment of periodontitis through a series of catalytic reactions. Reproduced with permission from ref. 184, copyright 2022, Elsevier. (d) Schematic of Ag-TiO₂ SAzymes with anti-SARS-CoV₂ activity. Ag-TiO₂ SAzymes adsorb onto the receptor binding domain (RBD) of spike 1 protein of SARS-CoV₂ containing abundant cysteine and asparagine to generate the SAzyme/virus complex, which can be phagocytosed by macrophages and colocalized with lysosomes. Reproduced with permission from ref. 185, copyright 2021, Elsevier.

In addition to copper, other metal SAzymes also show effective antibacterial activity. Yang's group prepared a g-ZnN₄-MoS₂ SAzyme via electrostatic interactions, which can be

applied to sonodynamic ion therapy to upgrade the antibacterial efficacy.¹⁸³ Benefiting from the synergetic regulation of the Zn single-atom and MoS₂ quantum dots, charge transfer and spin-flip were enhanced at the heterogeneous interfaces, which promoted the generation of singlet ¹O₂ from O₂ owing to a reduced activation energy of O₂. It has been shown that ¹O₂ can kill *S. aureus* with an antibacterial efficiency of 99.58% under 20 min of ultrasound irradiation. The excellent sonodynamic antibacterial efficiency and osteoinduction ability of g-ZnN₄-MoS₂ suggested attractive applications in ultrasonic antimicrobe. Another similar instance is a Pt SAzyme modified porphyrin MOF (PCN-222-Pt), where the active sites exhibit strong OXD- and POD-like activities and can lower the desorption energy of O₂ and produce ROS (Figure 12c). It displays an excellent anti-biofilm performance to deactivate bacteria at an inactivation efficiency of *S. aureus* and *E. coli* of 98.69% and 99.91%, respectively.¹⁸⁴

SAzymes possess not only prominent bactericidal activity, but also play a vital role as high-efficiency catalysts in antiviral research. Notably, Wang et al.¹⁸⁵ prepared Ag-TiO₂ SAzymes to combat SARS-CoV₂ coronavirus, which is currently posing a serious threat to global public health. The materials were rationally designed through a combination of ingenious experimental engineering and theoretical calculations, and exhibited a high POD-like activity (Figure 12d). Scanning electron microscopy (SEM) measurements showed that the SAzyme adsorbed onto the receptor binding domain (RBD) of the spike 1 protein of SARS-CoV₂ that contained abundant cysteine and asparagine via strong interactions with the Ag centers. The SAzyme/virus complex was then phagocytosed by macrophages and colocalized with lysosomes which supplied an appropriate acid condition for enzyme activity. Compared with traditional TiO₂ or Ag nanomaterial, Ag-TiO₂ SAzyme exhibited a much higher adsorption efficacy (99.65%) of SARS-CoV₂ pseudovirus. This demonstrated the great potential of SAzymes in antiviral applications.

5.4 Other applications

SAzymes have also been successfully applied in food safety monitoring,¹⁸⁶⁻¹⁸⁹ environmental survey,¹⁹⁰⁻¹⁹³ cytoprotection,^{194, 195} wound healing,¹⁹⁶ nervous system diseases therapy and brain trauma,¹⁹⁷⁻²⁰⁰ as well as drug dosing guides and outcome predictions. For instance, Ce-N-C SAzymes have been utilized for food safety monitoring and detection of pesticide residues, where the POD-like activity provided a colorimetric route to efficiently detect organophosphorus and carbamate pesticide residues via cascade reactions with AChE. The Ce SAzyme was integrated with bioactive paper using the 3D printing technology.²⁰¹ Mechanistically, TMB were oxidized to blue oxTMB, which was then reduced to colorless TMB by choline in the presence of Ce-N-C SAzyme and hydrogen peroxide. However, organophosphorus and carbamate pesticide residues could inhibit the activity of AChE and produce little or no choline, blocking the reverse reduction reaction. The color of bioactive paper was correlated with the pesticide residue content, allowing for the rapid portable detection of pesticides. Furthermore, Yang's group found that

hemin-loaded Zn-N-C SAzymes possessed an intrinsic POD-like activity, which could be used for rapid detection of propylgallate and formaldehyde in food samples.²⁰² The POD-like activity led to the oxidation of colorless propylgallate to yellow products while HCHO could inhibit propylgallate oxidation, leading to an apparent decrease in optical absorbance.

In addition, SAzymes exhibit antibacterial activity against a broad range of marine microorganisms and can act as promising anti-biofouling agents. Sun et al. developed a Co SAzyme with Co single atoms loaded into polyacrylamidoxime (PAO).²⁰³ The Co-PAO SAzyme catalyzed the generation of ROS from hydrogen peroxide and destruction of marine fouling biological entities, such as marine bacteria and marine algae.

Furthermore, as the abundant ROS generated by oxidative stress can damage brain tissue and induce a series of neuroinflammation, leading to the occurrence of various central nervous system (CNS) diseases, select SAzymes have also been found to exhibit satisfactory ROS-scavenging activity and great potential for the treatment of CNS diseases.²⁰⁴ For instance, ultrasmall carbon dots-supported Fe SAzyme (Fe-CDs) could serve as a kind of nontoxic nanomedicine to modulate tumor microenvironment via ROS regulation and lysosome-mediated autophagy.²⁰⁵ It has six naturally occurring enzymatic properties, OXD, CAT, SOD, and the POD family (HRP, GPx, and thiol peroxidase), that induce a cascade of reactions in vivo. In addition, the blood-brain barrier permeability and the ability to selectively target GBM in vivo can be greatly enhanced by peptide modification on the surface of Fe-CDs. Benefiting from the multiple enzyme-mimic properties and minimal toxicity, the Fe-CDs SAzymes possess a great potential in precise therapy of drug-resistant glioblastoma (GBM). Recently, Zhang et al. observed an ultrahigh biological activity of RhN₄, VN₄, and FeCuN₆ SAzymes through precise atomic engineering. The RhN₄ and VN₄ SAzymes formed an Rh/V-O-N₄ active site, displaying 4- and 5-fold higher affinity in POD-like performance than the FeN₄ and natural HRP. The RhN₄ structure also showed a CAT-like activity that was 20 times higher than that of the natural enzyme, while the VN₄ structure possessed a high GPx-like activity 7 times higher than that of the natural counterpart. The FeCuN₆ also showed an excellent SOD-like activity. These catalytic activities can be combined to construct novel healing sutures for brain trauma by promoting the vascular endothelial growth factor, regulating the immune cells like macrophages, and diminishing inflammation.²⁰⁶

6. Conclusion and Perspectives

SAzymes are a rising star in the field of catalysis and biomedicine, primarily because of multiple catalytic activities that mimic those of POD, OXD, CAT, and SOD, which can mediate the redox reactions between various substances, generating or scavenging ROS. In comparison to the easy degradation and high costs of natural enzymes and complicated structures and limited catalytic activity of conventional nanoparticle-based nanozymes, SAzymes

possesses excellent stability, well-defined central structure and low cost, leading to diverse applications in various fields. With homogeneously dispersed active sites and well-defined coordination structures of SAzymes, it has become possible to explore the correlation between the material structure and activity via rational regulation of the geometric and electronic structure. As highlighted in this review, there is no doubt that SAzymes, as emerging high-performance biocatalysts, will become promising alternatives to traditional enzymes for a range of biological/biomedical applications.

Yet, despite significant progresses, obstacles and challenges remain that hinder the further development of SAzymes. From the materials perspectives, most SAzymes are prepared by controlled pyrolysis of select precursors, where the carbon scaffolds typically exhibit a complex structure and aggregation of metal atoms inevitably occurs. The complexity of the materials structure renders it challenging to establish an unambiguous correlation between the materials structure and enzymatic activity. Thus, development of effective methods for the preparation of SAzymes with well-defined structures are urgently needed. This calls for a careful design of the precursors as well as deliberate manipulation of the thermal treatment conditions. Towards this end, ultrafast synthesis may be a viable option, where the ultrashort heating pulses can facilitate the retention of the organized structures of the precursors.²⁰⁷ In addition, one may take advantage of the latest breakthroughs in organometallic chemistry to pre-position the metal centers within a molecular framework.²⁰⁸ This will also be of particular importance when binuclear or even multinuclear atomic sites are desired.

From the biological perspective, while enzyme-like activities have been observed with SAzymes, the catalytic performance and substrate selectivity have remained mostly subpar as compared to natural enzymes. This is likely due to the high-order structure of the nanocomposites that deviates from the natural enzyme. With the advances of computing power and methods, the materials structure of the nanocomposite-based SAzymes can be optimized within the context of, for instance, covalency between the metal center and coordinating atoms, porosity of the structural scaffold, doping of heteroatoms, etc. In addition, thus far, the mechanistic insights into the interactions between SAzymes and biological targets have remained limited. This is particularly true with living microorganisms like bacterial cells and viruses, where the antimicrobial and antiviral activity may be a combined contribution of damages of the cell structural integrity and inhibition of the metabolism. In vivo imaging and spectroscopy analysis will be a key to unravelling the mechanistic details, which can be aided by low-temperature electron microscopy measurements.^{209, 210}

Author Contributions

Xueqian Xiao: Investigation, Writing – original draft; **Xiao Hu:** Investigation, Writing – original draft; **Qiming Liu:** Writing – review & editing; **Yulin Zhang:** Writing – original draft; **Guo-Jun Zhang:**

Resources, Writing – original draft; **Shaowei Chen**: Conceptualization, Resources, Writing – Review & editing.

Conflicts of interest

There are no conflicts to declare.

Acknowledgements

This work was supported, in part, by the National Science Foundation (CBET-1848841, CHE-1900235, and CHE-2003685)

References

- J. Bjerre, C. Rousseau, L. Marinescu and M. Bols, Artificial enzymes, "chemzymes": current state and perspectives, *Appl Microbiol Biotechnol*, 2008, **81**, 1-11.
- J. Wu, X. Wang, Q. Wang, Z. Lou, S. Li, Y. Zhu, L. Qin and H. Wei, Nanomaterials with enzyme-like characteristics (nanozymes): next-generation artificial enzymes (II), *Chem Soc Rev*, 2019, **48**, 1004-1076.
- L. Gao, J. Zhuang, L. Nie, J. Zhang, Y. Zhang, N. Gu, T. Wang, J. Feng, D. Yang, S. Perrett and X. Yan, Intrinsic peroxidase-like activity of ferromagnetic nanoparticles, *Nat Nanotechnol*, 2007, **2**, 577-583.
- F. Pogacean, C. Socaci, S. Pruneanu, A. R. Biris, M. Coros, L. Magerusan, G. Katona, R. Turcu and G. Borodi, Graphene based nanomaterials as chemical sensors for hydrogen peroxide – A comparison study of their intrinsic peroxidase catalytic behavior, *Sens Actuators B: Chem*, 2015, **213**, 474-483.
- R. Ragg, M. N. Tahir and W. Tremel, Solids Go Bio: Inorganic Nanoparticles as Enzyme Mimics, *Eur J Inorg Chem*, 2015, **2016**, 1906-1915.
- L. Gao and X. Yan, Nanozymes: an emerging field bridging nanotechnology and biology, *Sci China Life Sci*, 2016, **59**, 400-402.
- H. Wei and E. Wang, Nanomaterials with enzyme-like characteristics (nanozymes): next-generation artificial enzymes, *Chem Soc Rev*, 2013, **42**, 6060-6093.
- Y. Lin, J. Ren and X. Qu, Catalytically active nanomaterials: a promising candidate for artificial enzymes, *Acc Chem Res*, 2014, **47**, 1097-1105.
- Y. Ai, Z. N. Hu, X. Liang, H. b. Sun, H. Xin and Q. Liang, Recent Advances in Nanozymes: From Matters to Bioapplications, *Adv Funct Mater*, 2021, **32**, 2110432.
- A. P. Periasamy, P. Roy, W.-P. Wu, Y.-H. Huang and H.-T. Chang, Glucose Oxidase and Horseradish Peroxidase Like Activities of Cuprous Oxide/Polypyrrole Composites, *Electrochim Acta*, 2016, **215**, 253-260.
- D. Jiang, D. Ni, Z. T. Rosenkrans, P. Huang, X. Yan and W. Cai, Nanozyme: new horizons for responsive biomedical applications, *Chem Soc Rev*, 2019, **48**, 3683-3704.
- Y. Zhang, Y. Jin, H. Cui, X. Yan and K. Fan, Nanozyme-based catalytic theranostics, *RSC Adv*, 2019, **10**, 10-20.
- M. Liang and X. Yan, Nanozymes: From New Concepts, Mechanisms, and Standards to Applications, *Acc Chem Res*, 2019, **52**, 2190-2200.
- J. Han and J. Yoon, Supramolecular Nanozyme-Based Cancer Catalytic Therapy, *ACS Appl Bio Mater*, 2020, **3**, 7344-7351.
- C. Hong, X. Meng, J. He, K. Fan and X. Yan, Nanozyme: A promising tool from clinical diagnosis and environmental monitoring to wastewater treatment, *Particuology*, 2022, **71**, 90-107.
- L. Jiao, H. Yan, Y. Wu, W. Gu, C. Zhu, D. Du and Y. Lin, When Nanozymes Meet Single-Atom Catalysis, *Angew Chem Int Ed*, 2020, **59**, 2565-2576.
- X. Zhang, G. Li, G. Chen, D. Wu, X. Zhou and Y. Wu, Single-atom nanozymes: A rising star for biosensing and biomedicine, *Coord Chem Rev*, 2020, **418**, 213376.
- W. Wu, L. Huang, E. Wang and S. Dong, Atomic engineering of single-atom nanozymes for enzyme-like catalysis, *Chem Sci*, 2020, **11**, 9741-9756.
- C. Zhao, C. Xiong, X. Liu, M. Qiao, Z. Li, T. Yuan, J. Wang, Y. Qu, X. Wang, F. Zhou, Q. Xu, S. Wang, M. Chen, W. Wang, Y. Li, T. Yao, Y. Wu and Y. Li, Unraveling the enzyme-like activity of heterogeneous single atom catalyst, *Chem Commun*, 2019, **55**, 2285-2288.
- J. Pei, R. Zhao, X. Mu, J. Wang, C. Liu and X. D. Zhang, Single-atom nanozymes for biological applications, *Biomater Sci*, 2020, **8**, 6428-6441.
- R. Zhang, K. Fan and X. Yan, Nanozymes: created by learning from nature, *Sci China Life Sci*, 2020, **63**, 1183-1200.
- V. Kandathil and S. A. Patil, Single-atom nanozymes and environmental catalysis: A perspective, *Adv Colloid Interface Sci*, 2021, **294**, 102485.
- L. Su, S. Qin, Z. Xie, L. Wang, K. Khan, A. K. Tareen, D. Li and H. Zhang, Multi-enzyme activity nanozymes for biosensing and disease treatment, *Coord Chem Rev*, 2022, **473**, 214784.
- D. Xu, L. Wu, H. Yao and L. Zhao, Catalase-Like Nanozymes: Classification, Catalytic Mechanisms, and Their Applications, *Small*, 2022, **18**, e2203400.
- W. Yang, X. Yang, L. Zhu, H. Chu, X. Li and W. Xu, Nanozymes: Activity origin, catalytic mechanism, and biological application, *Coord Chem Rev*, 2021, **448**, 214170.
- F. Cao, L. Zhang, Y. You, L. Zheng, J. Ren and X. Qu, An Enzyme-Mimicking Single-Atom Catalyst as an Efficient Multiple Reactive Oxygen and Nitrogen Species Scavenger for Sepsis Management, *Angew Chem Int Ed*, 2020, **59**, 5108-5115.
- Y. Chen, H. Zou, B. Yan, X. Wu, W. Cao, Y. Qian, L. Zheng and G. Yang, Atomically Dispersed Cu Nanozyme with Intensive Ascorbate Peroxidase Mimic Activity Capable of Alleviating ROS-Mediated Oxidation Damage, *Adv Sci*, 2022, **9**, e2103977.
- Y. Chong, Q. Liu and C. Ge, Advances in oxidase-mimicking nanozymes: Classification, activity regulation and biomedical applications, *Nano Today*, 2021, **37**, 101076.
- C. Jiang, T. He, Q. Tang, J. He, Q. Ren, D.-Y. Zhang, B. Gurram, N. T. Blum, Y. Chen, P. Huang and J. Lin, Nanozyme catalyzed cascade reaction for enhanced chemodynamic therapy of low-H₂O₂ tumor, *Appl Mater Today*, 2022, **26**, 101357.
- D. Li, D. Dai, G. Xiong, S. Lan and C. Zhang, Metal-Based Nanozymes with Multienzyme-Like Activities as Therapeutic Candidates: Applications, Mechanisms, and Optimization Strategy, *Small*, 2022, DOI: 10.1002/smll.202205870, e2205870.
- P. Zhu, X. Xiong and D. Wang, Regulations of active moiety in single atom catalysts for electrochemical hydrogen evolution reaction, *Nano Res*, 2022, **15**, 5792-5815.
- M. Zandieh and J. Liu, Nanozyme Catalytic Turnover and Self-Limited Reactions, *ACS Nano*, 2021, **15**, 15645-15655.
- R. Li and D. Wang, Understanding the structure-performance relationship of active sites at atomic scale, *Nano Res*, 2022, **15**,

- 6888-6923.
34. Y. Huang, J. Ren and X. Qu, Nanozymes: Classification, Catalytic Mechanisms, Activity Regulation, and Applications, *Chem Rev*, 2019, **119**, 4357-4412.
35. X. Hai, S. Xi, S. Mitchell, K. Harrath, H. Xu, D. F. Akl, D. Kong, J. Li, Z. Li, T. Sun, H. Yang, Y. Cui, C. Su, X. Zhao, J. Li, J. Perez-Ramirez and J. Lu, Scalable two-step annealing method for preparing ultra-high-density single-atom catalyst libraries, *Nat Nanotechnol*, 2022, **17**, 174-181.
36. F. Meng, P. Zhu, L. Yang, L. Xia and H. Liu, Nanozymes with atomically dispersed metal centers: Structure–activity relationships and biomedical applications, *Chem Eng J*, 2023, **452**, 139411.
37. Q. Shi, T. Yu, R. Wu and J. Liu, Metal-Support Interactions of Single-Atom Catalysts for Biomedical Applications, *ACS Appl Mater Interfaces*, 2021, **13**, 60815-60836.
38. N. Cheng and X. Sun, Single atom catalyst by atomic layer deposition technique, *Chin J Catal*, 2017, **38**, 1508-1514.
39. H. Yan, Y. Lin, H. Wu, W. Zhang, Z. Sun, H. Cheng, W. Liu, C. Wang, J. Li, X. Huang, T. Yao, J. Yang, S. Wei and J. Lu, Bottom-up precise synthesis of stable platinum dimers on graphene, *Nat Commun*, 2017, **8**, 1070.
40. C. H. Choi, M. Kim, H. C. Kwon, S. J. Cho, S. Yun, H. T. Kim, K. J. Mayrhofer, H. Kim and M. Choi, Tuning selectivity of electrochemical reactions by atomically dispersed platinum catalyst, *Nat Commun*, 2016, **7**, 10922.
41. T. Gan, Q. He, H. Zhang, H. Xiao, Y. Liu, Y. Zhang, X. He and H. Ji, Unveiling the kilogram-scale gold single-atom catalysts via ball milling for preferential oxidation of CO in excess hydrogen, *Chem Eng J*, 2020, **389**, 124490.
42. Y. Wu, L. Jiao, X. Luo, W. Xu, X. Wei, H. Wang, H. Yan, W. Gu, B. Z. Xu, D. Du, Y. Lin and C. Zhu, Oxidase-Like Fe-N-C Single-Atom Nanozymes for the Detection of Acetylcholinesterase Activity, *Small*, 2019, **15**, 1903108.
43. Y. Zou, S. A. Kazemi, G. Shi, J. Liu, Y. Yang, N. M. Bedford, K. Fan, Y. Xu, H. Fu, M. Dong, M. Al-Mamun, Y. L. Zhong, H. Yin, Y. Wang, P. Liu and H. Zhao, Ruthenium single-atom modulated Ti3C2Tx MXene for efficient alkaline electrocatalytic hydrogen production, *EcoMat*, 2022, **5**, e12274.
44. M. A. Denchy, L. Wang, B. R. Bilik, L. Hansen, S. Albornoz, F. Lizano, N. Blando, Z. Hicks, G. Gantefoer and K. H. Bowen, Ultrasmall Cluster Model for Investigating Single Atom Catalysis: Dehydrogenation of 1-Propanamine by Size-Selected Pt(1)Zr(2)O(7) Clusters Supported on HOPG, *J Phys Chem A*, 2022, **126**, 7578-7590.
45. W. E. Kaden, T. Wu, W. A. Kunkel and S. L. Anderson, Electronic structure controls reactivity of size-selected Pd clusters adsorbed on TiO2 surfaces, *Science*, 2009, **326**, 826-829.
46. W. Fu, J. Wan, H. Zhang, J. Li, W. Chen, Y. Li, Z. Guo and Y. Wang, Photoinduced loading of electron-rich Cu single atoms by moderate coordination for hydrogen evolution, *Nat Commun*, 2022, **13**, 5496.
47. H. Wei, K. Huang, D. Wang, R. Zhang, B. Ge, J. Ma, B. Wen, S. Zhang, Q. Li, M. Lei, C. Zhang, J. Irawan, L. M. Liu and H. Wu, Iced photochemical reduction to synthesize atomically dispersed metals by suppressing nanocrystal growth, *Nat Commun*, 2017, **8**, 1490.
48. S. Ding, H.-A. Chen, O. Mekasuwandumrong, M. J. Hülsey, X. Fu, Q. He, J. Panpranot, C.-M. Yang and N. Yan, High-temperature flame spray pyrolysis induced stabilization of Pt single-atom catalysts, *Appl Catal B: Environ*, 2021, **281**, 119471.
49. A. A. Vernekar, D. Sinha, S. Srivastava, P. U. Paramasivam, P. D'Silva and G. Mughes, An antioxidant nanozyme that uncovers the cytoprotective potential of vanadia nanowires, *Nat Commun*, 2014, **5**, 5301.
50. Y. Suda, N. Hosoya and K. Miki, Si submonolayer and monolayer digital growth operation techniques using Si2H6 as atomically controlled growth nanotechnology, *Appl Surf Sci*, 2003, **216**, 424-430.
51. G. Vile, D. Albani, M. Nachtegaal, Z. Chen, D. Dontsova, M. Antonietti, N. Lopez and J. Perez-Ramirez, A stable single-site palladium catalyst for hydrogenations, *Angew Chem Int Ed Engl*, 2015, **54**, 11265-11269.
52. Y. Fan, S. Liu, Y. Yi, H. Rong and J. Zhang, Catalytic Nanomaterials toward Atomic Levels for Biomedical Applications: From Metal Clusters to Single-Atom Catalysts, *ACS Nano*, 2021, **15**, 2005-2037.
53. H. Song, M. Zhang and W. Tong, Single-Atom Nanozymes: Fabrication, Characterization, Surface Modification and Applications of ROS Scavenging and Antibacterial, *Molecules*, 2022, **27**, 5426.
54. A. Han, B. Wang, A. Kumar, Y. Qin, J. Jin, X. Wang, C. Yang, B. Dong, Y. Jia, J. Liu and X. Sun, Recent Advances for MOF-Derived Carbon-Supported Single-Atom Catalysts, *Small Methods*, 2019, **3**, 1800471.
55. B. Xu, S. Li, L. Zheng, Y. Liu, A. Han, J. Zhang, Z. Huang, H. Xie, K. Fan, L. Gao and H. Liu, A Bioinspired Five-Coordinated Single-Atom Iron Nanozyme for Tumor Catalytic Therapy, *Adv Mater*, 2022, **34**, e2107088.
56. S. Chen, W. Lu, R. Xu, J. Tan and X. Liu, Pyrolysis-free and universal synthesis of metal-NC single-atom nanozymes with dual catalytic sites for cytoprotection, *Carbon*, 2023, **201**, 439-448.
57. Q. Wang, D. Zhang, Y. Chen, W.-F. Fu and X.-J. Lv, Single-Atom Catalysts for Photocatalytic Reactions, *ACS Sustain Chem Eng*, 2019, **7**, 6430-6443.
58. H. Xiang, W. Feng and Y. Chen, Single-Atom Catalysts in Catalytic Biomedicine, *Adv Mater*, 2020, **32**, 1905994.
59. J. Wu, L. Xiong, B. Zhao, M. Liu and L. Huang, Densely Populated Single Atom Catalysts, *Small Methods*, 2019, **4**, 1900540.
60. Y. Chen, Q. Yuchi, T. Li, G. Yang, J. Miao, C. Huang, J. Liu, A. Li, Y. Qin and L. Zhang, Precise engineering of ultra-thin Fe2O3 decorated Pt-based nanozymes via atomic layer deposition to switch off undesired activity for enhanced sensing performance, *Sens Actuators B: Chem*, 2020, **305**, 127436.
61. F. Qin, J. Zhang, Z. Zhou, H. Xu, L. Cui, Z. Lv and Y. Qin, TiO2 Nanoflowers Decorated with FeOx Nanocluster and Single Atoms by Atomic Layer Deposition for Peroxidase-Mimicking Nanozymes, *ACS Appl Nano Mater*, 2022, **5**, 13090-13099.
62. J. H. Kim, D. Shin, J. Lee, D. S. Baek, T. J. Shin, Y. T. Kim, H. Y. Jeong, J. H. Kwak, H. Kim and S. H. Joo, A General Strategy to Atomically Dispersed Precious Metal Catalysts for Unravelling Their Catalytic Trends for Oxygen Reduction Reaction, *ACS Nano*, 2020, **14**, 1990-2001.
63. Q. Zhou, J. Cai, Z. Zhang, R. Gao, B. Chen, G. Wen, L. Zhao, Y. Deng, H. Dou, X. Gong, Y. Zhang, Y. Hu, A. Yu, X. Sui, Z. Wang and Z. Chen, A Gas-Phase Migration Strategy to Synthesize Atomically Dispersed Mn-N-C Catalysts for Zn-Air Batteries, *Small Methods*, 2021, **5**, 2100024.
64. L. Shen, D. Ye, H. Zhao and J. Zhang, Perspectives for Single-Atom Nanozymes: Advanced Synthesis, Functional Mechanisms, and Biomedical Applications, *Anal Chem*, 2021,

- 93**, 1221-1231.
65. T. Gao, Z. Zhu, Y. Li, H. Hu, H. Rong, W. Liu, T. Yang and X. Zhang, Highly efficient electromagnetic absorption on ZnN₄-based MOFs-derived carbon composites, *Carbon*, 2021, **177**, 44-51.
 66. X. Liu, F. He, Y. Lu, S. Wang, C. Zhao, S. Wang, X. Duan, H. Zhang, X. Zhao, H. Sun, J. Zhang and S. Wang, The double-edged effect of single atom metals on photocatalysis, *Chem Eng J*, 2023, **453**, 139833.
 67. E. Luo, H. Zhang, X. Wang, L. Gao, L. Gong, T. Zhao, Z. Jin, J. Ge, Z. Jiang, C. Liu and W. Xing, Single-Atom Cr-N(4) Sites Designed for Durable Oxygen Reduction Catalysis in Acid Media, *Angew Chem Int Ed Engl*, 2019, **58**, 12469-12475.
 68. L. Yan, L. Xie, X. L. Wu, M. Qian, J. Chen, Y. Zhong and Y. Hu, Precise regulation of pyrrole-type single-atom Mn-N₄ sites for superior pH-universal oxygen reduction, *Carbon Energy*, 2021, **3**, 856-865.
 69. M. Zhang, C. Lai, B. Li, S. Liu, D. Huang, F. Xu, X. Liu, L. Qin, Y. Fu, L. Li, H. Yi and L. Chen, MXenes as Superexcellent Support for Confining Single Atom: Properties, Synthesis, and Electrocatalytic Applications, *Small*, 2021, **17**, e2007113.
 70. N. Cheng, J. C. Li, D. Liu, Y. Lin and D. Du, Single-Atom Nanozyme Based on Nanoengineered Fe-N-C Catalyst with Superior Peroxidase-Like Activity for Ultrasensitive Bioassays, *Small*, 2019, **15**, e1901485.
 71. M. S. Kim, J. Lee, H. S. Kim, A. Cho, K. H. Shim, T. N. Le, S. S. A. An, J. W. Han, M. I. Kim and J. Lee, Heme Cofactor-Resembling Fe-N Single Site Embedded Graphene as Nanozymes to Selectively Detect H₂O₂ with High Sensitivity, *Adv Funct Mater*, 2019, **30**, 1905410.
 72. G. Balraj, R. Gurrapu, A. Anil Kumar, V. Sumalatha and D. Ayodhya, Facile synthesis and characterization of noble metals decorated g-C₃N₄ (g-C₃N₄/Pt and g-C₃N₄/Pd) nanocomposites for efficient photocatalytic production of Schiff bases, *Results Chem*, 2022, **4**, 100597.
 73. F. K. Kessler, Y. Zheng, D. Schwarz, C. Merschjann, W. Schnick, X. Wang and M. J. Bojdys, Functional carbon nitride materials – design strategies for electrochemical devices, *Nat Rev Materials*, 2017, **2**, 17030 (12017).
 74. S.-F. Duan, C.-L. Tao, Y.-Y. Geng, X.-Q. Yao, X.-W. Kang, J.-Z. Su, I. Rodríguez-Gutiérrez, M. Kan, M. Romero, Y. Sun, Y.-X. Zhao, D.-D. Qin and Y. Yan, Phosphorus-doped Isotype g-C₃N₄/g-C₃N₄: An Efficient Charge Transfer System for Photoelectrochemical Water Oxidation, *ChemCatChem*, 2019, **11**, 729-736.
 75. Y. Meng, L. Zhang, H. Jiu, Q. Zhang, H. Zhang, W. Ren, Y. Sun and D. Li, Construction of g-C₃N₄/ZIF-67 photocatalyst with enhanced photocatalytic CO₂ reduction activity, *Mater Sci Semicond Proc*, 2019, **95**, 35-41.
 76. T. Saberi Safaei, A. Mephah, X. Zheng, Y. Pang, C. T. Dinh, M. Liu, D. Sinton, S. O. Kelley and E. H. Sargent, High-Density Nanosharp Microstructures Enable Efficient CO(2) Electroreduction, *Nano Lett*, 2016, **16**, 7224-7228.
 77. Y. Fan, W. Zhang, Y. Liu, Z. Zeng, X. Quan and H. Zhao, Three-Dimensional Branched Crystal Carbon Nitride with Enhanced Intrinsic Peroxidase-Like Activity: A Hypersensitive Platform for Colorimetric Detection, *ACS Appl Mater Interfaces*, 2019, **11**, 17467-17474.
 78. J. Jiang, Z. Xiong, H. Wang, G. Liao, S. Bai, J. Zou, P. Wu, P. Zhang and X. Li, Sulfur-doped g-C₃N₄/g-C₃N₄ isotype step-scheme heterojunction for photocatalytic H₂ evolution, *J Mater Sci Technol*, 2022, **118**, 15-24.
 79. Z. Wang, K. Dong, Z. Liu, Y. Zhang, Z. Chen, H. Sun, J. Ren and X. Qu, Activation of biologically relevant levels of reactive oxygen species by Au/g-C(3)N(4) hybrid nanozyme for bacteria killing and wound disinfection, *Biomaterials*, 2017, **113**, 145-157.
 80. Y. Li, Z. He, L. Liu, Y. Jiang, W.-J. Ong, Y. Duan, W. Ho and F. Dong, Inside-and-out modification of graphitic carbon nitride (g-C₃N₄) photocatalysts via defect engineering for energy and environmental science, *Nano Energy*, 2023, **105**, 108032.
 81. J. Xing, N. Wang, X. Li, J. Wang, M. Taiwaikuli, X. Huang, T. Wang, L. Zhou and H. Hao, Synthesis and modifications of g-C₃N₄-based materials and their applications in wastewater pollutants removal, *J Environ Chem Eng*, 2022, **10**, 108782.
 82. Y. Yang, F. Yang, Z. Li, N. Zhang and S. Hao, Z-scheme g-C₃N₄/C/S-g-C₃N₄ heterostructural nanotube with enhanced porous structure and visible light driven photocatalysis, *Microporous and Mesoporous Materials*, 2021, **314**, 110891.
 83. D. Wang and Y. Zhao, Single-atom engineering of metal-organic frameworks toward healthcare, *Chem*, 2021, **7**, 2635-2671.
 84. B. Xu, Z. Huang, Y. Liu, S. Li and H. Liu, MOF-based nanomedicines inspired by structures of natural active components, *Nano Today*, 2023, **48**, 101690.
 85. S. Nazri, M. Khajeh, A. R. Oveisi, R. Luque, E. Rodríguez-Castellón and M. Ghaffari-Moghaddam, Thiol-functionalized PCN-222 MOF for fast and selective extraction of gold ions from aqueous media, *Sep Purif Technol*, 2021, **259**, 118197.
 86. Z. Zhou, J. Zhang, S. Mukherjee, S. Hou, R. Khare, M. Döblinger, O. Tomanec, M. Otyepka, M. Koch, P. Gao, L. Zhou, W. Li and R. A. Fischer, Porphyrinic MOF derived Single-atom electrocatalyst enables methanol oxidation, *Chem Eng J*, 2022, **449**, 137888.
 87. Z. Wang, Q. Sun, B. Liu, Y. Kuang, A. Gulzar, F. He, S. Gai, P. Yang and J. Lin, Recent advances in porphyrin-based MOFs for cancer therapy and diagnosis therapy, *Coord Chem Rev*, 2021, **439**, 213945.
 88. W. Y. Gao, M. Chrzanowski and S. Ma, Metal-metalloporphyrin frameworks: a resurging class of functional materials, *Chem Soc Rev*, 2014, **43**, 5841-5866.
 89. G. Zhan, Q. Xu, Z. Zhang, Z. Wei, T. Yong, N. Bie, X. Zhang, X. Li, J. Li, L. Gan and X. Yang, Biomimetic sonodynamic therapy-nanovaccine integration platform potentiates Anti-PD-1 therapy in hypoxic tumors, *Nano Today*, 2021, **38**, 101195.
 90. S. Daliran, A. R. Oveisi, Y. Peng, A. Lopez-Magano, M. Khajeh, R. Mas-Balleste, J. Aleman, R. Luque and H. Garcia, Correction: Metal-organic framework (MOF)-, covalent-organic framework (COF)-, and porous-organic polymers (POP)-catalyzed selective C-H bond activation and functionalization reactions, *Chem Soc Rev*, 2022, **51**, 8140.
 91. Z. Li, S. Qiu, Y. Song, S. Huang, J. Gao, L. Sun and J. Hou, Engineering single-atom active sites anchored covalent organic frameworks for efficient metallaphotoredox CN cross-coupling reactions, *Sci Bull*, 2022, **67**, 1971-1981.
 92. P. Dong, Y. Wang, A. Zhang, T. Cheng, X. Xi and J. Zhang, Platinum Single Atoms Anchored on a Covalent Organic Framework: Boosting Active Sites for Photocatalytic Hydrogen Evolution, *ACS Catal*, 2021, **11**, 13266-13279.
 93. K. Chi, Y. Wu, X. Wang, Q. Zhang, W. Gao, L. Yang, X. Chen, D. Chang, Y. Zhang, T. Shen, X. Lu, Y. Zhao and Y. Liu, Single Atom Catalysts with Out-of-Plane Coordination Structure on Conjugated Covalent Organic Frameworks, *Small*, 2022, **18**, e2203966.
 94. Z. Dong, L. Zhang, J. Gong and Q. Zhao, Covalent organic

- framework nanorods bearing single Cu sites for efficient photocatalysis, *Chem Eng J*, 2021, **403**, 126383.
95. M. Kou, W. Liu, Y. Wang, J. Huang, Y. Chen, Y. Zhou, Y. Chen, M. Ma, K. Lei, H. Xie, P. K. Wong and L. Ye, Photocatalytic CO₂ conversion over single-atom MoN₂ sites of covalent organic framework, *Appl Catal B: Environ*, 2021, **291**, 120146.
96. Q. Tang, S. Cao, T. Ma, X. Xiang, H. Luo, P. Borovskikh, R. D. Rodriguez, Q. Guo, L. Qiu and C. Cheng, Engineering Biofunctional Enzyme-Mimics for Catalytic Therapeutics and Diagnostics, *Adv Funct Mater*, 2020, **31**, 2007475.
97. M. Abbas and M. A. Z. G. Sial, New Horizon in stabilization of single atoms on metal-oxide supports for CO₂ reduction, *Nano Mater Sci*, 2021, **3**, 368-389.
98. B. Han, Y. Guo, Y. Huang, W. Xi, J. Xu, J. Luo, H. Qi, Y. Ren, X. Liu, B. Qiao and T. Zhang, Strong Metal-Support Interactions between Pt Single Atoms and TiO₂, *Angew Chem Int Ed*, 2020, **59**, 11824-11829.
99. Z. Liu, L. Sun, Q. Zhang, Z. Teng, H. Sun and C. Su, TiO₂-supported Single-atom Catalysts: Synthesis, Structure, and Application, *Chem Res Chin Univ*, 2022, **38**, 1123-1138.
100. Y.-Q. Su, Y. Wang, J.-X. Liu, I. A. W. Filot, K. Alexopoulos, L. Zhang, V. Muravev, B. Zijlstra, D. G. Vlachos and E. J. M. Hensen, Theoretical Approach To Predict the Stability of Supported Single-Atom Catalysts, *ACS Catal*, 2019, **9**, 3289-3297.
101. X. Liao, Y. Zhao, C. Liu, X. Li, Y. Sun, K. Kato, M. Yamauchi and Z. Jiang, Low temperature surface oxygen activation in crystalline MnO₂ triggered by lattice confined Pd single atoms, *J Energy Chem*, 2021, **62**, 136-144.
102. Y. Wang, K. Qi, S. Yu, G. Jia, Z. Cheng, L. Zheng, Q. Wu, Q. Bao, Q. Wang, J. Zhao, X. Cui and W. Zheng, Revealing the Intrinsic Peroxidase-Like Catalytic Mechanism of Heterogeneous Single-Atom Co-MoS₂, *Nanomicro Lett*, 2019, **11**, 102.
103. B. Chang, L. Zhang, S. Wu, Z. Sun and Z. Cheng, Engineering single-atom catalysts toward biomedical applications, *Chem Soc Rev*, 2022, **51**, 3688-3734.
104. X. Wei, S. Song, W. Song, W. Xu, L. Jiao, X. Luo, N. Wu, H. Yan, X. Wang, W. Gu, L. Zheng and C. Zhu, Fe(3)C-Assisted Single Atomic Fe Sites for Sensitive Electrochemical Biosensing, *Anal Chem*, 2021, **93**, 5334-5342.
105. F. Wu, C. Pan, C. T. He, Y. Han, W. Ma, H. Wei, W. Ji, W. Chen, J. Mao, P. Yu, D. Wang, L. Mao and Y. Li, Single-Atom Co-N(4) Electrocatalyst Enabling Four-Electron Oxygen Reduction with Enhanced Hydrogen Peroxide Tolerance for Selective Sensing, *J Am Chem Soc*, 2020, **142**, 16861-16867.
106. B. Jiang and M. Liang, Advances in Single-Atom Nanozymes Research†, *Chin J Chem*, 2020, **39**, 174-180.
107. S. Fu, C. Zhu, D. Su, J. Song, S. Yao, S. Feng, M. H. Engelhard, D. Du and Y. Lin, Porous Carbon-Hosted Atomically Dispersed Iron-Nitrogen Moiety as Enhanced Electrocatalysts for Oxygen Reduction Reaction in a Wide Range of pH, *Small*, 2018, **14**, e1703118.
108. X. Niu, Q. Shi, W. Zhu, D. Liu, H. Tian, S. Fu, N. Cheng, S. Li, J. N. Smith, D. Du and Y. Lin, Unprecedented peroxidase-mimicking activity of single-atom nanozyme with atomically dispersed Fe-N(x) moieties hosted by MOF derived porous carbon, *Biosens Bioelectron*, 2019, **142**, 111495.
109. W. Liu, L. Chu, C. Zhang, P. Ni, Y. Jiang, B. Wang, Y. Lu and C. Chen, Hemin-assisted synthesis of peroxidase-like Fe-N-C nanozymes for detection of ascorbic acid-generating bio-enzymes, *Chem Eng J*, 2021, **415**, 128876.
110. Y. Feng, J. Qin, Y. Zhou, Q. Yue and J. Wei, Spherical mesoporous Fe-N-C single-atom nanozyme for photothermal and catalytic synergistic antibacterial therapy, *J Colloid Interface Sci*, 2022, **606**, 826-836.
111. X. Wu, Y. Sun, T. He, Y. Zhang, G. J. Zhang, Q. Liu and S. Chen, Iron, Nitrogen-Doped Carbon Aerogels for Fluorescent and Electrochemical Dual-Mode Detection of Glucose, *Langmuir*, 2021, **37**, 11309-11315.
112. Liang, Huang, Jinxing, Chen, Linfeng, Gan, Jin, Wang, Shaojun and Dong, Single-atom nanozymes, *Science Advances*, 2019, **5**, 46.
113. Q. Chen, X. Zhang, S. Li, J. Tan, C. Xu and Y. Huang, MOF-derived Co₃O₄@Co-Fe oxide double-shelled nanocages as multi-functional specific peroxidase-like nanozyme catalysts for chemo/biosensing and dye degradation, *Chem Eng J*, 2020, **395**, 125130.
114. B. Liu, Y. Xue, Z. Gao, K. Tang, G. Wang, Z. Chen and X. Zuo, Antioxidant identification using a colorimetric sensor array based on Co-N-C nanozyme, *Colloids Surf B Biointerfaces*, 2021, **208**, 112060.
115. L. Sun, Y. Yan, S. Chen, Z. Zhou, W. Tao, C. Li, Y. Feng and F. Wang, Co-N-C single-atom nanozymes with oxidase-like activity for highly sensitive detection of biothiols, *Anal Bioanal Chem*, 2022, **414**, 1857-1865.
116. S. Cai, J. Liu, J. Ding, Z. Fu, H. Li, Y. Xiong, Z. Lian, R. Yang and C. Chen, Tumor-Microenvironment-Responsive Cascade Reactions by a Cobalt-Single-Atom Nanozyme for Synergistic Nanocatalytic Chemotherapy, *Angew Chem Int Ed*, 2022, **61**, e202204502.
117. Y. Song, T. He, Y. Zhang, C. Yin, Y. Chen, Q. Liu, Y. Zhang and S. Chen, Cobalt single atom sites in carbon aerogels for ultrasensitive enzyme-free electrochemical detection of glucose, *J Electroanal Chem*, 2022, **906**, 116024.
118. B. Xu, H. Wang, W. Wang, L. Gao, S. Li, X. Pan, H. Wang, H. Yang, X. Meng, Q. Wu, L. Zheng, S. Chen, X. Shi, K. Fan, X. Yan and H. Liu, A Single-Atom Nanozyme for Wound Disinfection Applications, *Angew Chem Int Ed*, 2019, **58**, 4911-4916.
119. Z. Li, B. Li and C. Yu, Atomic Aerogel Materials (or single atom aerogels): an Interesting New Paradigm in Materials Science and Catalysis Science, *Adv Mater*, 2023, DOI: 10.1002/adma.202211221, e2211221.
120. C. B. Ma, Y. Xu, L. Wu, Q. Wang, J. J. Zheng, G. Ren, X. Wang, X. Gao, M. Zhou, M. Wang and H. Wei, Guided Synthesis of a Mo/Zn Dual Single-Atom Nanozyme with Synergistic Effect and Peroxidase-like Activity, *Angew Chem Int Ed*, 2022, **61**, e202116170.
121. Y. Kong, Y. Li, X. Sang, B. Yang, Z. Li, S. Zheng, Q. Zhang, S. Yao, X. Yang, L. Lei, S. Zhou, G. Wu and Y. Hou, Atomically Dispersed Zinc(II) Active Sites to Accelerate Nitrogen Reduction Kinetics for Ammonia Electrosynthesis, *Adv Mater*, 2022, **34**, e2103548.
122. K. S. Siddiqi, A. Ur Rahman, Tajuddin and A. Husen, Properties of Zinc Oxide Nanoparticles and Their Activity Against Microbes, *Nanoscale Res Lett*, 2018, **13**, 141.
123. B. Qiao, A. Wang, X. Yang, L. F. Allard, Z. Jiang, Y. Cui, J. Liu, J. Li and T. Zhang, Single-atom catalysis of CO oxidation using Pt₁/FeO_x, *Nat Chem*, 2011, **3**, 634-641.
124. Y. Xin, N. Zhang, Y. Lv, J. Wang, Q. Li and Z. Zhang, From nanoparticles to single atoms for Pt/CeO₂: Synthetic strategies, characterizations and applications, *J Rare Earths*, 2020, **38**, 850-862.
125. X. Ye, H. Wang, Y. Lin, X. Liu, L. Cao, J. Gu and J. Lu, Insight of the stability and activity of platinum single atoms on ceria, *Nano Res*, 2019, **12**, 1401-1409.

126. R. Yan, S. Sun, J. Yang, W. Long, J. Wang, X. Mu, Q. Li, W. Hao, S. Zhang, H. Liu, Y. Gao, L. Ouyang, J. Chen, S. Liu, X. D. Zhang and D. Ming, Nanozyme-Based Bandage with Single-Atom Catalysis for Brain Trauma, *ACS Nano*, 2019, **13**, 11552-11560.
127. Y. Chen, P. Wang, H. Hao, J. Hong, H. Li, S. Ji, A. Li, R. Gao, J. Dong, X. Han, M. Liang, D. Wang and Y. Li, Thermal Atomization of Platinum Nanoparticles into Single Atoms: An Effective Strategy for Engineering High-Performance Nanozymes, *J Am Chem Soc*, 2021, **143**, 18643-18651.
128. Y. Fan, X. Gan, H. Zhao, Z. Zeng, W. You and X. Quan, Multiple application of SAzyme based on carbon nitride nanorod-supported Pt single-atom for H₂O₂ detection, antibiotic detection and antibacterial therapy, *Chem Eng J*, 2022, **427**, 131572.
129. S. H. Chang, B. Y. Chen and J. X. Lin, Toxicity assessment and selective leaching characteristics of Cu-Al-Ni shape memory alloys in biomaterials applications, *J Appl Biomater Funct Mater*, 2016, **14**, e59-64.
130. J. Zhu, Q. Li, X. Li, X. Wu, T. Yuan and Y. Yang, Simulated Enzyme Activity and Efficient Antibacterial Activity of Copper-Doped Single-Atom Nanozymes, *Langmuir*, 2022, **38**, 6860-6870.
131. G. Song, J. C. Li, Z. Majid, W. Xu, X. He, Z. Yao, Y. Luo, K. Huang and N. Cheng, Phosphatase-like activity of single-atom CeNC nanozyme for rapid detection of Al(3), *Food Chem*, 2022, **390**, 133127.
132. C. Mochizuki, Y. Inomata, S. Yasumura, M. Lin, A. Taketoshi, T. Honma, N. Sakaguchi, M. Haruta, K.-i. Shimizu, T. Ishida and T. Murayama, Defective NiO as a Stabilizer for Au Single-Atom Catalysts, *ACS Catal*, 2022, DOI: 10.1021/acscatal.2c00108, 6149-6158.
133. C. Rong, X. Shen, Y. Wang, L. Thomsen, T. Zhao, Y. Li, X. Lu, R. Amal and C. Zhao, Electronic Structure Engineering of Single-Atom Ru Sites via Co-N₄ Sites for Bifunctional pH-Universal Water Splitting, *Adv Mater*, 2022, **34**, 2110103.
134. R. Tian, H. Ma, W. Ye, Y. Li, S. Wang, Z. Zhang, S. Liu, M. Zang, J. Hou, J. Xu, Q. Luo, H. Sun, F. Bai, Y. Yang and J. Liu, Se-Containing MOF Coated Dual-Fe-Atom Nanozymes With Multi-Enzyme Cascade Activities Protect Against Cerebral Ischemic Reperfusion Injury, *Adv Funct Mater*, 2022, **32**, 2204025.
135. M. Fan, J. Cui, J. Wu, R. Vajtai, D. Sun and P. M. Ajayan, Improving the Catalytic Activity of Carbon-Supported Single Atom Catalysts by Polynary Metal or Heteroatom Doping, *Small*, 2020, **16**, e1906782.
136. S. Ji, B. Jiang, H. Hao, Y. Chen, J. Dong, Y. Mao, Z. Zhang, R. Gao, W. Chen, R. Zhang, Q. Liang, H. Li, S. Liu, Y. Wang, Q. Zhang, L. Gu, D. Duan, M. Liang, D. Wang, X. Yan and Y. Li, Matching the kinetics of natural enzymes with a single-atom iron nanozyme, *Nat Catal*, 2021, **4**, 407-417.
137. R. Li, X. He, R. Javed, J. Cai, H. Cao, X. Liu, Q. Chen, D. Ye and H. Zhao, Switching on-off-on colorimetric sensor based on Fe-N/S-C single-atom nanozyme for ultrasensitive and multimodal detection of Hg(2), *Sci Total Environ*, 2022, **834**, 155428.
138. C.-C. Hou, H.-F. Wang, C. Li and Q. Xu, From metal-organic frameworks to single/dual-atom and cluster metal catalysts for energy applications, *Energy Environ Sci*, 2020, **13**, 1658-1693.
139. Q. Chen, Y. Liu, Y. Lu, Y. Hou, X. Zhang, W. Shi and Y. Huang, Atomically dispersed Fe/Bi dual active sites single-atom nanozymes for cascade catalysis and peroxydisulfate activation to degrade dyes, *J Hazard Mater*, 2022, **422**, 126929.
140. G. Darabdhara, J. Bordoloi, P. Manna and M. R. Das, Biocompatible bimetallic Au-Ni doped graphitic carbon nitride sheets: A novel peroxidase-mimicking artificial enzyme for rapid and highly sensitive colorimetric detection of glucose, *Sens Actuators B: Chem*, 2019, **285**, 277-290.
141. H. Zhang and N. Toshima, Fabrication of catalytically active AgAu bimetallic nanoparticles by physical mixture of small Au clusters with Ag ions, *Appl Catal A: Gen*, 2012, **447-448**, 81-88.
142. Y. Wang, Z. Zhang, G. Jia, L. Zheng, J. Zhao and X. Cui, Elucidating the mechanism of the structure-dependent enzymatic activity of Fe-N/C oxidase mimics, *Chem Commun*, 2019, **55**, 5271-5274.
143. J. Chen, L. Huang, Q. Wang, W. Wu, H. Zhang, Y. Fang and S. Dong, Bio-inspired nanozyme: a hydratase mimic in a zeolitic imidazolate framework, *Nanoscale*, 2019, **11**, 5960-5966.
144. H. Liang, F. Lin, Z. Zhang, B. Liu, S. Jiang, Q. Yuan and J. Liu, Multicopper Laccase Mimicking Nanozymes with Nucleotides as Ligands, *ACS Appl Mater Interfaces*, 2017, **9**, 1352-1360.
145. J. Li, W. Liu, X. Wu and X. Gao, Mechanism of pH-switchable peroxidase and catalase-like activities of gold, silver, platinum and palladium, *Biomaterials*, 2015, **48**, 37-44.
146. P. Yin, T. Yao, Y. Wu, L. Zheng, Y. Lin, W. Liu, H. Ju, J. Zhu, X. Hong, Z. Deng, G. Zhou, S. Wei and Y. Li, Single Cobalt Atoms with Precise N-Coordination as Superior Oxygen Reduction Reaction Catalysts, *Angew Chem Int Ed*, 2016, **55**, 10800-10805.
147. M. Lu, C. Wang, Y. Ding, M. Peng, W. Zhang, K. Li, W. Wei and Y. Lin, Fe-N/C single-atom catalysts exhibiting multienzyme activity and ROS scavenging ability in cells, *Chem Commun (Camb)*, 2019, **55**, 14534-14537.
148. Y. Wang, R. Du, L. Y. S. Lee and K. Y. Wong, Rational design and structural engineering of heterogeneous single-atom nanozyme for biosensing, *Biosens Bioelectron*, 2022, **216**, 114662.
149. G. Song, Q. Zhang, S. Liang, Y. Yao, M. Feng, Z. Majid, X. He, K. Huang, J.-C. Li and N. Cheng, Oxidation activity modulation of a single atom Ce-N-C nanozyme enabling a time-resolved sensor to detect Fe³⁺ and Cr⁶⁺, *J Mater Chem C*, 2022, **10**, 15656-15663.
150. X. Zhou, M. Wang, J. Chen, X. Xie and X. Su, Peroxidase-like activity of Fe-N-C single-atom nanozyme based colorimetric detection of galactose, *Anal Chim Acta*, 2020, **1128**, 72-79.
151. H. Yan, L. Jiao, H. Wang, Y. Zhu, Y. Chen, L. Shuai, M. Gu, M. Qiu, W. Gu and C. Zhu, Single-atom Bi-anchored Au hydrogels with specifically boosted peroxidase-like activity for cascade catalysis and sensing, *Sens Actuators B: Chem*, 2021, **343**, 130108.
152. S. Wang, Z. Hu, Q. Wei, H. Zhang, W. Tang, Y. Sun, H. Duan, Z. Dai, Q. Liu and X. Zheng, Diatomic active sites nanozymes: Enhanced peroxidase-like activity for dopamine and intracellular H₂O₂ detection, *Nano Res*, 2022, **15**, 4266-4273.
153. M. Feng, Q. Zhang, X. Chen, D. Deng, X. Xie and X. Yang, Controllable synthesis of boron-doped Zn-N-C single-atom nanozymes for the ultrasensitive colorimetric detection of p-phenylenediamine, *Biosens Bioelectron*, 2022, **210**, 114294.
154. W. Wu, L. Huang, X. Zhu, J. Chen, D. Chao, M. Li, S. Wu and S. Dong, Reversible inhibition of the oxidase-like activity of Fe single-atom nanozymes for drug detection, *Chem Sci*, 2022, **13**, 4566-4572.
155. F. X. Hu, T. Hu, S. Chen, D. Wang, Q. Rao, Y. Liu, F. Dai, C. Guo, H. B. Yang and C. M. Li, Single-Atom Cobalt-Based Electrochemical Biomimetic Uric Acid Sensor with Wide Linear Range and Ultralow Detection Limit, *Nano-Micro Letters*, 2020,

- 13, 1-13.
156. Y. Liu, P. Zhao, Y. Liang, Y. Chen, J. Pu, J. Wu, Y. Yang, Y. Ma, Z. Huang, H. Luo, D. Huo and C. Hou, Single-atom nanozymes Co-N-C as an electrochemical sensor for detection of bioactive molecules, *Talanta*, 2023, **254**, 124171.
157. Q. H. Nguyen, D. H. Lee, P. T. Nguyen, P. G. Le and M. I. Kim, Foldable paper microfluidic device based on single iron site-containing hydrogel nanozyme for efficient glucose biosensing, *Chem Eng J*, 2023, **454**, 140541.
158. W. Wu, S. Xia, Y. Liu, C. Ma, Z. Lyu, M. Zhao, S. Ding and Q. Hu, Single-atom catalysts with peroxidase-like activity boost gel-sol transition-based biosensing, *Biosens Bioelectron*, 2023, **225**, 115112.
159. S. Li, D. Liu, B. Wu, H. Sun, X. Liu, H. Zhang, N. Ding and L. Wu, One-pot synthesis of a peroxidase-like nanozyme and its application in visual assay for tyrosinase activity, *Talanta*, 2022, **239**, 123088.
160. M. Wang, L. Liu, X. Xie, X. Zhou, Z. Lin and X. Su, Single-atom iron containing nanozyme with peroxidase-like activity and copper nanoclusters based ratio fluorescent strategy for acetylcholinesterase activity sensing, *Sens Actuators B: Chem*, 2020, **313**, 128023.
161. X. Niu, N. Cheng, X. Ruan, D. Du and Y. Lin, Review—Nanozyme-Based Immunosensors and Immunoassays: Recent Developments and Future Trends, *J Electrochem Soc*, 2019, **167**.
162. L. Sun, C. Li, Y. Yan, Y. Yu, H. Zhao, Z. Zhou, F. Wang and Y. Feng, Engineering DNA/Fe-N-C single-atom nanozymes interface for colorimetric biosensing of cancer cells, *Anal Chim Acta*, 2021, **1180**, 338856.
163. B. Jiang, Z. Guo and M. Liang, Recent progress in single-atom nanozymes research, *Nano Res*, 2022, DOI: 10.1007/s12274-022-4856-7, 1-12.
164. D. Wang, H. Wu, S. Z. F. Phua, G. Yang, W. Qi Lim, L. Gu, C. Qian, H. Wang, Z. Guo, H. Chen and Y. Zhao, Self-assembled single-atom nanozyme for enhanced photodynamic therapy treatment of tumor, *Nat Commun*, 2020, **11**, 357.
165. M. Chang, Z. Hou, M. Wang, C. Yang, R. Wang, F. Li, D. Liu, T. Peng, C. Li and J. Lin, Single-Atom Pd Nanozyme for Ferroptosis-Boosted Mild-Temperature Photothermal Therapy, *Angew Chem Int Ed*, 2021, **60**, 12971-12979.
166. Y. Zou, B. Jin, H. Li, X. Wu, Y. Liu, H. Zhao, D. Zhong, L. Wang, W. Chen, M. Wen and Y. N. Liu, Cold Nanozyme for Precise Enzymatic Antitumor Immunity, *ACS Nano*, 2022, **16**, 21491-21504.
167. Y. Zhu, W. Wang, P. Gong, Y. Zhao, Y. Pan, J. Zou, R. Ao, J. Wang, H. Cai, H. Huang, M. Yu, H. Wang, L. Lin, X. Chen and Y. Wu, Enhancing Catalytic Activity of a Nickel Single Atom Enzyme by Polynary Heteroatom Doping for Ferroptosis-Based Tumor Therapy, *ACS Nano*, 2023, DOI: 10.1021/acsnano.2c11923, 3064-3076.
168. B. Lin, H. Chen, D. Liang, W. Lin, X. Qi, H. Liu and X. Deng, Acidic pH and High-H₂O₂ Dual Tumor Microenvironment-Responsive Nanocatalytic Graphene Oxide for Cancer Selective Therapy and Recognition, *ACS Appl Mater Interfaces*, 2019, **11**, 11157-11166.
169. H. He, Z. Fei, T. Guo, Y. Hou, D. Li, K. Wang, F. Ren, K. Fan, D. Zhou, C. Xie, C. Wang and X. Lu, Bioadhesive injectable hydrogel with phenolic carbon quantum dot supported Pd single atom nanozymes as a localized immunomodulation niche for cancer catalytic immunotherapy, *Biomaterials*, 2022, **280**, 121272.
170. N. Feng, Q. Li, Q. Bai, S. Xu, J. Shi, B. Liu and J. Guo, Development of an Au-anchored Fe Single-atom nanozyme for biocatalysis and enhanced tumor photothermal therapy, *J Colloid Interface Sci*, 2022, **618**, 68-77.
171. Y. Zhu, W. Wang, J. Cheng, Y. Qu, Y. Dai, M. Liu, J. Yu, C. Wang, H. Wang, S. Wang, C. Zhao, Y. Wu and Y. Liu, Stimuli-Responsive Manganese Single-Atom Nanozyme for Tumor Therapy via Integrated Cascade Reactions, *Angew Chem Int Ed*, 2021, **60**, 9480-9488.
172. Y. Xing, J. Xiu, M. Zhou, T. Xu, M. Zhang, H. Li, X. Li, X. Du, T. Ma and X. Zhang, Copper Single-Atom Jellyfish-like Nanomotors for Enhanced Tumor Penetration and Nanocatalytic Therapy, *ACS Nano*, 2023, DOI: 10.1021/acsnano.3c00076.
173. T. Li, L. Chen, X. Fu, Z. Liu, S. Zhu, Y. Chen and J. Zhang, Iron Single-Atom nanocatalysts in response to tumor microenvironment for highly efficient Chemo-chemodynamic therapy, *J Ind Eng Chem*, 2022, **112**, 210-217.
174. Q. Chen, M. Zhang, H. Huang, C. Dong, X. Dai, G. Feng, L. Lin, D. Sun, D. Yang, L. Xie, Y. Chen, J. Guo and X. Jing, Single Atom-Doped Nanosensitizers for Mutually Optimized Sono/Chemo-Nanodynamic Therapy of Triple Negative Breast Cancer, *Adv Sci*, 2023, **10**, e2206244.
175. S. Wang, M. Ma, Q. Liang, X. Wu, K. Abbas, J. Zhu, Q. Xu, A. C. Tedesco and H. Bi, Single-Atom Manganese Anchored on Carbon Dots for Promoting Mitochondrial Targeting and Photodynamic Effect in Cancer Treatment, *ACS Appl Nano Mater*, 2022, **5**, 6679-6690.
176. Y. Xing, L. Li, Y. Chen, L. Wang, S. Tang, X. Xie, S. Wang, J. Huang, K. Cai and J. Zhang, Flower-like Nanozyme with Highly Porous Carbon Matrix Induces Robust Oxidative Storm against Drug-Resistant Cancer, *ACS Nano*, 2023, DOI: 10.1021/acsnano.2c12698.
177. F. Mo, M. Zhang, X. Duan, C. Lin, D. Sun and T. You, Recent Advances in Nanozymes for Bacteria-Infected Wound Therapy, *Int J Nanomedicine*, 2022, **17**, 5947-5990.
178. M. D. Rojas-Andrade, G. Chata, D. Rouholiman, J. L. Liu, C. Saltikov and S. W. Chen, Antibacterial mechanisms of graphene-based composite nanomaterials, *Nanoscale*, 2017, **9**, 994-1006.
179. C. Jin, S. Fan, Z. Zhuang and Y. Zhou, Single-atom nanozymes: From bench to bedside, *Nano Res*, 2022, DOI: 10.1007/s12274-022-5060-5, 1-11.
180. Y. Zhao, Y. Yu, F. Gao, Z. Wang, W. Chen, C. Chen, J. Yang, Y. Yao, J. Du, C. Zhao and Y. Wu, A highly accessible copper single-atom catalyst for wound antibacterial application, *Nano Res*, 2021, **14**, 4808-4813.
181. X. Wang, Q. Shi, Z. Zha, D. Zhu, L. Zheng, L. Shi, X. Wei, L. Lian, K. Wu and L. Cheng, Copper single-atom catalysts with photothermal performance and enhanced nanozyme activity for bacteria-infected wound therapy, *Bioact Mater*, 2021, **6**, 4389-4401.
182. F. Meng, M. Peng, Y. Chen, X. Cai, F. Huang, L. Yang, X. Liu, T. Li, X. Wen, N. Wang, D. Xiao, H. Jiang, L. Xia, H. Liu and D. Ma, Defect-rich graphene stabilized atomically dispersed Cu₃ clusters with enhanced oxidase-like activity for antibacterial applications, *Appl Catal B: Environ*, 2022, **301**, 120826.
183. X. Feng, J. Lei, L. Ma, Q. Ouyang, Y. Zeng, H. Liang, C. Lei, G. Li, L. Tan, X. Liu and C. Yang, Ultrasonic Interfacial Engineering of MoS₂-Modified Zn Single-Atom Catalysts for Efficient Osteomyelitis Sonodynamic Ion Therapy, *Small*, 2022, **18**, e2105775.
184. Y. Yu, Y. Cheng, L. Tan, X. Liu, Z. Li, Y. Zheng, T. Wu, Y. Liang, Z.

- Cui, S. Zhu and S. Wu, Theory-screened MOF-based single-atom catalysts for facile and effective therapy of biofilm-induced periodontitis, *Chem Eng J*, 2022, **431**, 133279.
185. D. Wang, B. Zhang, H. Ding, D. Liu, J. Xiang, X. J. Gao, X. Chen, Z. Li, L. Yang, H. Duan, J. Zheng, Z. Liu, B. Jiang, Y. Liu, N. Xie, H. Zhang, X. Yan, K. Fan and G. Nie, TiO₂ supported single Ag atoms nanozyme for elimination of SARS-CoV₂, *Nano Today*, 2021, **40**, 101243.
186. H. Li, M. Sun, H. Gu, J. Huang, G. Wang, R. Tan, R. Wu, X. Zhang, S. Liu, L. Zheng, W. Chen and Z. Chen, Peroxidase-Like FeCoZn Triple-Atom Catalyst-Based Electronic Tongue for Colorimetric Discrimination of Food Preservatives, *Small*, 2023, DOI: 10.1002/sml.202207036, e2207036.
187. Y. Mao, S. Gao, L. Yao, L. Wang, H. Qu, Y. Wu, Y. Chen and L. Zheng, Single-atom nanozyme enabled fast and highly sensitive colorimetric detection of Cr(VI), *J Hazard Mater*, 2021, **408**, 124898.
188. A. Payal, S. Krishnamoorthy, A. Elumalai, J. A. Moses and C. Anandharamkrishnan, A Review on Recent Developments and Applications of Nanozymes in Food Safety and Quality Analysis, *Food Anal Methods*, 2021, **14**, 1537-1558.
189. F. Zhang, Y. Li, X. Li, R. Liu, Y. Sang, X. Wang and S. Wang, Nanozyme-enabled sensing strategies for determining the total antioxidant capacity of food samples, *Food Chem*, 2022, **384**, 132412.
190. E. Ko, W. Hur, S. E. Son, G. H. Seong and D. K. Han, Au nanoparticle-hydrogel nanozyme-based colorimetric detection for on-site monitoring of mercury in river water, *Mikrochim Acta*, 2021, **188**, 382.
191. Y. Tian, Y. Chen, M. Chen, Z. L. Song, B. Xiong and X. B. Zhang, Peroxidase-like Au@Pt nanozyme as an integrated nanosensor for Ag(+) detection by LSPR spectroscopy, *Talanta*, 2021, **221**, 121627.
192. H. Yang, X. Wu, L. Su, Y. Ma, N. J. D. Graham and W. Yu, The Fe-N-C oxidase-like nanozyme used for catalytic oxidation of NOM in surface water, *Water Res*, 2020, **171**, 115491.
193. Z. Zhou, M. Li, C. Kuai, Y. Zhang, V. F. Smith, F. Lin, A. Aiello, D. P. Durkin, H. Chen and D. Shuai, Fe-based single-atom catalysis for oxidizing contaminants of emerging concern by activating peroxides, *J Hazard Mater*, 2021, **418**, 126294.
194. Y. Ai, J. You, J. Gao, J. Wang, H.-b. Sun, M. Ding and Q. Liang, Multi-shell nanocomposites based multienzyme mimetics for efficient intracellular antioxidation, *Nano Res*, 2021, **14**, 2644-2653.
195. L. Sun, W. Li, Z. Liu, Z. Zhou and Y. Feng, Iodine-doped single-atom cobalt catalysts with boosted antioxidant enzyme-like activity for colitis therapy, *Chem Eng J*, 2023, **453**, 139870.
196. Q. Xu, Y. Hua, Y. Zhang, M. Lv, H. Wang, Y. Pi, J. Xie, C. Wang and Y. Yong, A Biofilm Microenvironment-Activated Single-Atom Iron Nanozyme with NIR-Controllable Nanocatalytic Activities for Synergetic Bacteria-Infected Wound Therapy, *Adv Healthc Mater*, 2021, **10**, e2101374.
197. K. Chen, S. Sun, J. Wang and X.-D. Zhang, Catalytic nanozymes for central nervous system disease, *Coord Chem Rev*, 2021, **432**, 213751.
198. X. Gao, W. Ma, J. Mao, C. T. He, W. Ji, Z. Chen, W. Chen, W. Wu, P. Yu and L. Mao, A single-atom Cu-N(2) catalyst eliminates oxygen interference for electrochemical sensing of hydrogen peroxide in a living animal brain, *Chem Sci*, 2021, **12**, 15045-15053.
199. Z. Lyu, S. Ding, N. Zhang, Y. Zhou, N. Cheng, M. Wang, M. Xu, Z. Feng, X. Niu, Y. Cheng, C. Zhang, D. Du and Y. Lin, Single-Atom Nanozymes Linked Immunosorbent Assay for Sensitive Detection of Abeta 1-40: A Biomarker of Alzheimer's Disease, *Research*, 2020, **2020**, 4724505.
200. B. Yan, F. Wang, S. He, W. Liu, C. Zhang, C. Chen and Y. Lu, Peroxidase-like activity of Ru-N-C nanozymes in colorimetric assay of acetylcholinesterase activity, *Anal Chim Acta*, 2022, **1191**, 339362.
201. G. Song, J. Zhang, H. Huang, X. Wang, X. He, Y. Luo, J. C. Li, K. Huang and N. Cheng, Single-atom Ce-N-C nanozyme bioactive paper with a 3D-printed platform for rapid detection of organophosphorus and carbamate pesticide residues, *Food Chem*, 2022, **387**, 132896.
202. H. Li, Q. Li, Q. Shi, Y. Wang, X. Liu, H. Tian, X. Wang, D. Yang and Y. Yang, Hemin loaded Zn-N-C single-atom nanozymes for assay of propyl gallate and formaldehyde in food samples, *Food Chem*, 2022, **389**, 132985.
203. W. Sun, L. Feng, J. Zhang, K. Lin, H. Wang, B. Yan, T. Feng, M. Cao, T. Liu, Y. Yuan and N. Wang, Amidoxime Group-Anchored Single Cobalt Atoms for Anti-Biofouling during Uranium Extraction from Seawater, *Adv Sci*, 2022, **9**, e2105008.
204. W. Wei, Single-atom nanozymes towards central nervous system diseases, *Nano Res*, 2022, DOI: 10.1007/s12274-022-5104-x, 1-19.
205. P. Muhammad, S. Hanif, J. Li, A. Guller, F. U. Rehman, M. Ismail, D. Zhang, X. Yan, K. Fan and B. Shi, Carbon dots supported single Fe atom nanozyme for drug-resistant glioblastoma therapy by activating autophagy-lysosome pathway, *Nano Today*, 2022, **45**, 101530.
206. S. Zhang, Y. Li, S. Sun, L. Liu, X. Mu, S. Liu, M. Jiao, X. Chen, K. Chen, H. Ma, T. Li, X. Liu, H. Wang, J. Zhang, J. Yang and X. D. Zhang, Single-atom nanozymes catalytically surpassing naturally occurring enzymes as sustained stitching for brain trauma, *Nat Commun*, 2022, **13**, 4744.
207. Q. M. Liu and S. W. Chen, Ultrafast synthesis of electrocatalysts, *Trends Chem*, 2022, **4**, 918-934.
208. T. He, Y. Song, Y. Chen, X. Song, B. Lu, Q. Liu, H. Liu, Y. Zhang, X. Ouyang and S. Chen, Atomically dispersed ruthenium in carbon aerogels as effective catalysts for pH-universal hydrogen evolution reaction, *Chem Eng J*, 2022, **442**, 136337.
209. R. N. Burton-Smith and K. Murata, Cryo-electron microscopy of the giant viruses, *Microscopy (Oxf)*, 2021, **70**, 477-486.
210. J. H. Chen, W. Wang, C. Wang, T. Kuang, J. R. Shen and X. Zhang, Cryo-electron microscopy structure of the intact photosynthetic light-harvesting antenna-reaction center complex from a green sulfur bacterium, *J Integr Plant Biol*, 2023, **65**, 223-234.